

Descriptive analysis of dental X-ray images using various practical methods: A review

Anuj Kumar^{Corresp., 1}, Harvendra Singh Bhadauria¹, Annapurna Singh¹

¹ Computer Science & Engineering, Govind Ballabh Pant Institute of Engineering & Technology, Pauri Garhwal, Uttarakhand, India

Corresponding Author: Anuj Kumar
Email address: dranujdhiman@gmail.com

In dentistry, practitioners interpret various dental X-ray imaging modalities to identify tooth-related problems, abnormalities, or teeth structures changes. Another aspect of dental imaging is that it can be helpful in the field of biometrics. Human dental image analysis is a challenging and time-consuming task due to the unspecified and uneven structures of various teeth, and hence the manual investigation of dental abnormalities is at par excellence. However, automation in the field of dental image segmentation and analysis is essentially the need of the hour in order to ensure error free diagnosis and better treatment planning. In this article, we have provided a comprehensive survey of dental image segmentation and analysis by investigating more than 130 research works conducted through various dental imaging modalities, such as various modes of X-ray, CT (Computed Tomography), CBCT (Cone Beam Computed Tomography), etc. Overall state-of-the-art research works have been classified into three major categories, i.e., image processing, machine learning, and deep learning approaches, and their respective advantages and limitations are identified and discussed. The survey presents extensive details of the state-of-the-art methods, including image modalities, pre-processing applied for image enhancement, performance measures, and datasets utilized.

Descriptive analysis of dental X-ray images using various practical methods: A review

Anuj Kumar^a, H S Bhadauria^a, Annapurna Singh^a

^aDepartment Computer Science & Engineering, Govind Ballabh Pant Institute of Engineering & Technology, Ghurdauri, Pauri Garhwal, Uttarakhand, India.

Abstract: In dentistry, practitioners interpret various dental X-ray imaging modalities to identify tooth-related problems, abnormalities, or teeth structures changes. Another aspect of dental imaging is that it can be helpful in the field of biometrics. Human dental image analysis is a challenging and time-consuming task due to the unspecified and uneven structures of various teeth, and hence the manual investigation of dental abnormalities is at par excellence. However, automation in the field of dental image segmentation and analysis is essentially the need of the hour in order to ensure error free diagnosis and better treatment planning. In this article, we have provided a comprehensive survey of dental image segmentation and analysis by investigating more than 130 research works conducted through various dental imaging modalities, such as various modes of X-ray, CT (Computed Tomography), CBCT (Cone Beam Computed Tomography), etc. Overall state-of-the-art research works have been classified into three major categories, i.e., image processing, machine learning, and deep learning approaches, and their respective advantages and limitations are identified and discussed. The survey presents extensive details of the state-of-the-art methods, including image modalities, pre-processing applied for image enhancement, performance measures, and datasets utilized.

Keywords: Dental X-ray, Machine Learning, Deep Learning, Convolutional Neural Networks

1. Introduction

Dental X-ray imaging (DXRI) has become a backbone to dentists across the globe because of the assistance provided in medical diagnosis (Oprea et al., 2008). Teeth X-rays are a significant imaging assessment that can provide doctors with a thorough clinical diagnosis and dental structures' preventive examinations (Molteni, 1993). The visual inspection has an abysmal sensitive rate; therefore, human screening may not identify a high proportion of caries (Olsen et al., 2009). Detection of disease is one of the most critical aspects of radiography. Furthermore, if there are a large number of X-rays to be analyzed, the process can be time-consuming, as with tooth structure analysis. In most cases, an automatic computerized tool that can aid in the investigation process would be highly beneficial. Dental image examination involved various stages consisting of image enhancement, segmentation, feature extractions, and identification of regions, which are subsequently valuable for detecting cavities, tooth fractures, cyst or tumor detection, root canal length, and growth tooth in children (Kutsch, 2011). Also, various studies mentioned that used for the analysis of dental imaging modalities are beneficial in applications like human identification, age estimation, biometrics, and so on (Caruso, Silvestri & Sconfienza, 2013).

Many image segmentation & classification methods have been proposed in recent years, but the DXRI analysis is still challenging and complicated because of X-ray images' disparities and not systematic way of capturing tooth X-rays. In dental imaging, segmentation plays an essential role in analyzing the dental radiographs as per the different goals and objectives (Said et al., 2004). Segmentation divides the teeth X-ray image into meaningful objects like identifying hidden teeth structures, bone loss, interproximal caries,

periodontal diseases, injuries, etc. (Shah et al., 2006). Various segmentation methods proposed by researchers and computer aided systems developed. Computer-aided systems are becoming more powerful and intelligent for identifying abnormalities after processing medical images (like X-rays, microscopic images, ultrasound images, and MRI images). In this article, we have compared various image processing, machine learning, and deep learning approaches to identify & analyze various dental structures using different X-ray imaging modalities. Also, specific benchmarks in the journey of DXRI methods are represented in Figure 1.

In the existing research work, DXRI categorized segmentation methods by threshold-based, boundary-based, cluster-based, region-based, or watershed-based (Rad et al., 2013; Subramanyam, Prasad & Anuradha, 2014; Silva, Oliveira & Pithon, 2018). However, In (Schwendicke et al., 2019) various techniques based on convolution neural network(CNN) for dental image segmentation are provided. In previous studies, researchers have suggested many approaches for DXRI segmentation. However, performance metrics, details of the databases, and different imaging modalities require to be investigated to a great extent (Silva, Oliveira & Pithon, 2018; Schwendicke et al., 2019).

1.1. A brief about dental imaging modalities

Dental imaging modalities provide information about teeth, bone regions, gums, soft tissues, minute details of tooth loss and injuries, and assisting in root canal therapy, which is not visible during a dentist's oral examination.

Dental imaging modalities are mainly classified as intra-oral and extra-oral X-ray images. Moreover, these images are extensively used in dentistry for medical diagnosis (Abrahams, 2001; Caruso, Silvestri & Sconfienza, 2013). Various Dental imaging modalities categorization based on intra-oral and extra-oral are shown in Figure 2.

Dental radiographs can discover problems in the mouth, jaws, teeth, bone loss, fractures, cysts at an early stage. X-rays can help in finding issues that can not be visualized with an oral assessment. Identifying and diagnosing problems earliest stage can save wealth, pain, and sometimes even individual life.

Types of dental radiography

Intra-oral radiography. An X-ray film is placed inside the mouth to capture the image, which comprises all the detailed information about tooth health, teeth arrangement, root canal infection, and identifying caries. Categories of intra-oral X-ray images are:

- **Periapical images.** It provides information of root and surrounding bone areas containing three to four teeth in the single X-ray image.
- **Bitewing images.** It generally helps in detecting the information of upper and lower tooth structures. This X-ray beam shows the dentist how these teeth are arranged with one another and how to spot a cavity between teeth. Bitewing X-rays may also be used to ensure the proper fit of a crown (a cap that completely encloses a tooth) or other restorations (such as bridges). It can also detect any rotting or disrupted dental fillings.
- **Occlusal images.** Occlusal X-rays provide insight into the mouth's base, revealing the upper or lower jaw's bite. They place a strong emphasis on children's tooth development and placement.

Extraoral radiography. In which, X-ray film is positioned outside the mouth to capture the entire skull and jaws region. Extraoral X-rays are classified into many types.

- **Panoramic X-rays** X-rays are full-sized and capture overall tooth structure. Also, the pictures provide information about the skull and jaw. These images are mainly used to examine fractures, trauma, jaws diseases, pathological lesions and evaluate the impacted teeth. These scans are less detailed than intraoral X-rays and are rarely used to diagnose cavities or root canal therapy. On the other hand, these images are used to assess the condition of impacted teeth, checkups, the relationship between teeth and jaws, inspect the bones of the face, and track development or advancement.
- **Cephalometric X-rays** also called ceph X-ray, depict the jaw's whole part, including the head's entire side. It is employed in both dentistry and medicine for diagnosis and clinical preparation purposes.
- **Sialogram** uses a substance that is infused into the salivary glands to make them visible on X-ray film. Doctors may prescribe this test to check for salivary gland issues, such as blockages or Sjogren's symptoms (a symptom condition involving the dry mouth and dry eyes; this condition may play a role in tooth decay).
- **Dental computed tomography(CT)** is an imaging technique that gives insights into 3-D internal structures. This kind of visualization is used to identify maladies such as cysts, cancers, and fractures in the face's bones.
- **Cone-beam computed tomography(CBCT)** generates precise and high-quality pictures. Cone beam CT is an X-ray type that generates 3D visions of dental formations, soft tissues, nerves, and bones. It helps in guiding the tooth implants and finding cyst and tumefaction in the mouth. It can also find issues in the gum areas, roots, and jaws structures. Cone beam CT is similar in some ways to standard dental CT.

In this survey, we have considered articles in which the researchers used techniques extensively applied to periapical, bitewing, panoramic, CT, CBCT, and photographic color images. Nowadays, digital X-ray imaging is emerging as a new research area with growing applications in a variety of fields.

1.2. Challenges faced by doctors in analyzing dental X-ray images

Dental practitioners used X-ray radiographs to examine dental anatomy and to determine the care strategy for the patient. Because of a lack of resources, X-ray interpretations rely more on the doctor's expertise, and this manual examination is a difficult task in dentistry (Wang et al., 2016). Therefore, computer-aided systems are introduced to reduce complexity and make the identification process easy and fast. Healthcare decision support systems developed to provide technical guidance to clinical decision-making experts in the health care field (Mendonça, 2004). These systems help identify and treat the earliest symptom of demineralization of tooth caries, root canal, and periodontal diseases.

This paper explores the potential computational methods used for developing computer-aided systems, identifies the challenges faced in their implementation, and provides future directions (Amer & Aqel, 2015; Wang et al., 2016). Automatic detection of abnormalities, anomalies, and abrupt changes in teeth structures is a big challenge for researchers. Here, we have addressed some of the tooth-related problems, which are still a challenge for the researchers to develop expert systems.

We worked together with a few dental practitioners to understand the set of common difficulties encountered by them. These problems are significantly related to cavities(or caries), root canal treatment

(RCT), cysts, teeth implants, and teeth growth. Working in collaboration with dentists helps computer science professionals and researchers to design & develop models that can solve dentists' problems during examination.

1.3. Brief descriptions of dental problems

Tooth Caries Enamel decay, also known as tooth cavity (or caries), may result from acid-producing bacteria in the mouth affecting tooth structures. Bacteria on the teeth are primarily found in the white or pale yellow plaque that forms on the teeth if they are not brushed regularly. Caries diagnosed mainly through the use of bitewing and periapical X-ray images. Caries classified into six classes, as illustrated in Figure 3, by G.V. Black (Black, 1981)(Wolff, Allen & Kaim, 2007).

Class I Cavity present on teeth' pits & fissures surface, which can be seen clinically (Class I refers to clinically visible surfaces of a posterior tooth—lingual/occlusal/buccal surfaces).

Class II Present on the tooth region's proximal surface may include two or more regions (Class II refers to a posterior tooth's surfaces that are not visible clinically).

Class III Cavity on incisor and canine proximal surfaces that does not include the incisal angle.

Class IV Caries was discovered on canine and incisor teeth' proximal surface when the incisal angle was taken into account.

Class V Caries is found near the gum line of teeth and is identified by decay near the tooth-gum junction.

Class VI These caries are discovered on the tooth surface's cusp tips and incisal corners.

Another classification of caries is given based on its severity (Iannucci & Howerton, 2012). As shown in Figure 4, the onset of interproximal caries can be classified as incipient, mild, advanced, or extreme, depending on the amount of enamel and dentin involved.

Incipient caries In which lesion just go halfway through the enamel.

Moderate Lesion that extends higher than midway through the enamel. However, it does not have the dentino-enamel junction (DEJ).

Advanced A lesion extending to or across the DEJ but not reaching more than half the distance to the pulp

Severe Lesion ranges through both enamel and dentin and extra than half the distance to the pulp.

Numerous researchers have proposed different image processing and machine learning methods to identify abnormalities in real-time dental X-ray image datasets. Hence, we are looking at some of the abnormalities present in teeth X-ray images to understand the intensity variations shown in Figure 5.

Root Canal Treatment (RCT) When there is an infection deep within the enamel, then RCT is used. A bacterial infection infected the pulp area inside the tooth. If the problem is not detected earlier, the infection will progress to a critical stage, requiring tooth removal. The dentist may also take a series of X-ray photographs of the affected tooth before performing a root canal procedure. It enables them to obtain a clean appearance of the root canal and assess the tooth's damaged area. However, This helps the dentist to immediately fill (or restore) the affected teeth. Figure 6 depicts some sample X-ray images taken during root canal treatment and diagnosed after treatment. Many researchers proposed methods to detect the root canal, but no one has given expected outcomes.

157

158 1.4. Contribution

159 DXRI analysis is an evolving and prospective research field, but still, there is a lack of systematic study
160 available except for one or two studies. The major contributions of this work are as follows:

- 161 1. A comprehensive survey consisting of more than 130 articles related to dental imaging techniques
162 for the last 15 years is presented.
- 163 2. Overall state-of-the-art research works have been classified into three major categories, i.e.,
164 image processing, machine learning, and deep learning approaches, and their respective
165 advantages and limitations are identified and discussed
- 166 3. A comprehensive review of dental imaging methods is provided in terms of various performance
167 measures and dental imaging databases used for implementation and generation.

168 This review structure organized as follows: Methodology is given in Sect. 2, and at last, the conclusion is
169 mentioned in Sect. 3.

170 2. Methodology

171 In this survey, we found 130 research articles from 2004 to 2020, as mentioned in Figure 8, that covered
172 almost all research articles from different online digital libraries like Springer, Elsevier, IEEE, and
173 Google Scholar. All these articles are conferences, Book chapters, peer-reviewed and reputed journals in
174 computer science and digital dental imaging. A total number of articles deliberating various imaging
175 modalities: Periapical, Bitewing, Panoramic, Hybrid, CT, CBCT, Photographic color teeth images, and
176 undefined datasets are given in Table 1.

177 In literature, various researchers have proposed methods for different types of applications. Methods are
178 categorized as image processing techniques given in section 2.1, conventional machine learning methods
179 given in section 2.3, and deep learning approaches provided in section 2.3. Also, methods are
180 characterized based on imaging modalities (periapical X-rays, bitewing X-rays, panoramic X-rays, CBCT
181 or CT images, etc.) as shown in Figure 7.

182 The research incorporated in this systematic review mainly focused on the use of medical image
183 processing and artificial intelligence (AI) for the detection and diagnosis of dental caries, periodontal
184 disease recognition, tooth arrangement and numbering, root canal detection, periapical lesions detection,
185 salivary gland disease diagnosis, cyst detection, osteoporosis detection, determining the growth and
186 development of deciduous teeth, identification and analysis of cephalometric landmarks, fracture
187 identification, etc.

188 *Standards for this review's studies*

189 Criteria for inclusion

- 190 1. The articles must be focused on different imaging modalities and their applications in dentistry.
- 191 2. In this survey, we have searched various online databases and found almost 130 articles covering
192 various approaches to make automatic identification systems in the field of dentistry.

3. The years of these studies were considered in order to research the progression of AI patterns in dentistry that have grown and changed over time.

2.1 Image processing methods for dental image analysis

The research adopts various image processing strategies for dental imaging to investigate the structures of teeth and caries present and classify abnormalities to help dentists prepare for the appropriate diagnosis. It involves various pre-processing, segmentation, and classification approaches to make an automatic dental identification system that makes doctors' work more accessible, unambiguous, and faster. A simple traditional model used for dental image processing is mentioned in Figure 9.

2.1.1 Pre-processing techniques

Dental imaging consists of different image modalities, and X-rays are the most common medical imaging method used to classify bone and hard tissues. In dentistry, dental imaging mainly refers to identifying fractures, teeth structures, jaws alignment, cyst, and bone loss, which has become tremendously popular in dental imaging (Goyal, Agrawal & Sohi, 2018). Noise level, artifacts, and image contrast are vital values that control an image's overall quality. Many pixel locations in the picture produce more photons than in others, and it looks brighter than other locations even though the strength of the photons is the same. The image quality obtained depends on varying factors such as the dynamic range of the sensors, the lighting conditions, distortion, and the artifact examined (Sarage & Jambhorkar, 2012). Interpretation of a low-resolution image is often a complex and time-consuming process. Pre-processing corrects the spatial resolution and local adjustment to improve the dark shadows' luminosity to maintain the input image's overall quality (Hossain, Alsharif & Yamashita, 2010). Enhancement and filtering techniques are used to enhance the overall image quality parameters before further processing. There has been an immense amount of literature about this, but we focused on the methods applied to digital dental imaging. In Table 2, image pre-processing techniques are addressed by various researchers to recuperate the quality of dental images.

Contrast stretching, Grayscale stretching, Log transformation, Gamma correction, image negative, and histogram equalization methods are standard enhancement methods to improve medical images' quality. X-rays are typically grayscale pictures, with high noise rates and low resolution. Thus, the image contrast and representation of boundary is relatively weak and small (Ramani, Vanitha & Valarmathy, 2013). Extracting features from these X-rays is quite a difficult task with very minimal details and a low-quality image. By adding specific contrast enhancement techniques significantly improves image quality. So that segmentation and extraction of features from such images can be performed more accurately and conveniently (Kushol et al., 2019). Therefore, a contrast stretching approach has been widely used to enhance digital X-rays' quality (Lai & Lin, 2008; Vijayakumari et al., 2012; Berdouses et al., 2015; Purnama et al., 2015; Avuçlu & Bacsıftçi, 2020). Adaptive local contrast stretching makes use of local homogeneity to solve the problem of over and under enhancement. One of the prominent methods to refine the contrast of the image is histogram equalization (HE) (Harandi & Pourghassem, 2011; Menon & Rajeshwari, 2016; Obuchowicz Rafałand Nurzynska et al., 2018; Banday & Mir, 2019). HE is the way of increasing the dynamic range of an image histogram and it also causes unrealistic impacts in images; however, it is very effective for scientific pictures such as satellite, Computed tomography, or X-rays. A

downside of the approach is its indiscriminate existence. This can increase ambient noise contrast while reducing the useful quality features of an image.

On the other hand, filtering methods applied to medical images help to eradicate the noise up to some extent. Gaussian, Poisson, and quantum noise are different types of noise artifacts usually found in X-Rays & CTs, particularly when the image is captured (Razifar et al., 2005; Goyal, Agrawal & Sohi, 2018). The noise-free images achieve the efficiency to get the best result and improve the test's precision. If we try to reduce one type of noise, it may disrupt the other. Various filters have been used to achieve the best potential outcome for the irregularities present in dental images like Average filter, Bilateral filter, Laplacian filter, homomorphic filter, and Butterworth filter, Median Gaussian filter, and Weiner filter. As we have analyzed in the survey, the Gaussian filter and the median filter used by various researchers which shows the best result compared to some others (Benyó et al., 2009; Prajapati, Desai & Modi, 2012; Nuansanong, Kiattisin & Leelasantitham, 2014; Razali et al., 2014; Datta & Chaki, 2015a,b; Rad et al., 2015; Tuan, Ngan & others, 2016; Jain & Chauhan, 2017; Alsmadi, 2018). However, the drawback of the median filter is that it degrades the boundary details. Whereas the Gaussian filter performs best in peak detection, the limitation is that it reduces the picture's information.

2.1.2 Dental image segmentation approaches used for different imaging modalities

Medical image segmentation is an essential step to find valuable information. Dental X-ray segmentation faces more difficulties as compared to other medical imaging modalities, which makes the segmentation more complicated or challenging, and various dental image problems are mentioned in Figure 10. The segmentation process refers to the localization of artifacts or the boundary tracing, analysis of structure, etc. Human eyes distinguish the objects of interest quickly and remove them from the background tissues, but it is a great challenge in developing algorithms. Furthermore, image segmentation has applications distinct from computer vision; it is often used to extract or exclude different portions of an image. General dental image segmentation methods are categorized as thresholding-based, contour or snake models, level set methods, clustering-based methods, and region growing (Rad et al., 2013). Moreover, there has been a significant number of surveys presented by various authors (Rad et al., 2013; Sharma, Rana & Kundra, 2015). However, none of them categorized the methods based on dental imaging modalities.

In this article, various segmentation and classification techniques are discussed and reviewed, considering multiple dental imaging modalities. In the field of dental imaging, the choice of selecting a correct algorithm for the particular image dataset is most important. This study explores image processing methods used explicitly for particular dental imaging modalities, as given in Table 3.

Bitewing X-rays are widely used by researchers for the application of human identification and biometrics. The human identification using X-rays is made by applying adaptive thresholding, iterative thresholding, and region growing approaches for the segmentation. In the next step, image features are extracted to archive and retrieve dental images used for human identification (Mahoor & Abdel-Mottaleb, 2004, 2005; Nomir & Abdel-Mottaleb, 2005, 2007, 2008; Zhou & Abdel-Mottaleb, 2005). In (Huang et al., 2012), missing tooth locations were detected with an adaptive windowing scheme combined with the isolation curve method, which shows the accuracy rate higher than (Nomir & Abdel-Mottaleb, 2005). (Pushparaj, Gurunathan & Arumugam, 2013) primarily aimed at estimating the shape of the entire tooth. In which segmentation is performed by applying horizontal and vertical integral projection. In addition,

teeth boundary was estimated using the fast connected component labeling algorithm, and lastly, Mahalanobis distance is measured for the matching.

Periapical X-rays help clinical diagnosis for dental caries and root canal regions by applying various image processing techniques (Oprea et al., 2008). Many times dentists use periapical X-ray images to spot caries lesions from dental X-rays. Regardless of human brain vision, it is often hard to correctly identify caries by manually examining the X-ray image. Caries detection methods for periapical X-rays have used iterative ways to isolate the initially suspected areas. Then, separated regions are subsequently analyzed. In (Rad et al., 2015), automatic caries identified by applying segmentation using k-means clustering and feature detection using GLCM. However, it shows image quality issues in some cases, and because of these issues, tooth detection may give a false result. (Singh & Agarwal, 2018) applied color masking techniques to mark the carious lesions to find the percentage value of the affected area.

Another approach (Osterloh & Viriri, 2019) mainly focused on upper and lower jaws separation with the help of thresholding and integral projection, and the learning model is employed to locate caries. This model shows better accuracy as compared with (Dykstra, 2008; Tracy et al., 2011; Valizadeh et al., 2015). In (Obuchowicz Rafał and Nurzynska et al., 2018), k-means clustering (CLU) and first-order features (FOF) were used to show the best performance for the identification of caries. However, this approach applied to the dataset of 10 patients with confirmed caries. A geodesic contour technique (Datta, Chaki & Modak, 2019) shows better computational time results than multilevel thresholding, watershed, and level set. However, this approach's limitation is that it does not work well for poor-quality pictures, which leads to inappropriate feature extraction. In (Datta, Chaki & Modak, 2020) proposed a method that reduced the computational efforts and caries region identified in optimum time. The X-ray image is processed in the neutrosophic domain to identify the suspicious part, and an active contour method is employed to extract the outer line of the carious part. The benefit of this method is that it prevents recursive iterations using neutrosophication during suspicious area detection.

The semi-automatic method for root canal length detection is proposed by (Harandi & Pourghassem, 2011; Purnama et al., 2015) to help dental practitioners properly treat root canal treatment (RCT). Periapical X-rays are also used for the automatic segmentation of cyst or abscess. (Devi, Banumathi & Ulaganathan, 2019) proposed a fully automatic hybrid approach that combined both feature-based isophote curvature and model-based fast marching method (FMM). It shows good accuracy and optimum results as compared to (Jain & Chauhan, 2017). Furthermore, various approaches were used to automatically detect teeth structures (Huang & Hsu, 2008; Sattar & Karray, 2012; Niroshika, Meegama & Fernando, 2013; Nuansanong, Kiattisin & Leelasantitham, 2014; Kumar, Bhadauria & Singh, 2020).

Panoramic X-rays help identify jaw fractures, the structure of jaws, and deciduous teeth. These X-rays are less detailed as compared to periapical and bitewing. Wavelet transformation-based segmentation of panoramic X-rays shows better results than adaptive and iterative thresholding (Patanachai, Covavisaruch & Sinthanayothin, 2010). A fully automatic segmentation of the teeth using the Template matching technique introduced by (Poonsri et al., 2016) but shows 50% matching accuracy results. In (Razali et al., 2014) analyzed X-rays for the age estimations by comparing edge detection approaches. (Amer & Aqel, 2015) have suggested a method used to extract wisdom teeth using the otsu threshold combined with morphological dilation. Then, connected component labeling extracts the jaws and teeth regions.

(Mahdi & Kobashi, 2018) sets multi-threshold by applying quantum particle swarm optimization to improve the accuracy. (Fariza et al., 2019) employed a method to extract dentin, enamel, pulp, and other surrounding dental structures using conditional spatial fuzzy C-means clustering. Subsequently, the performance improved as compared to inherently used FCM approaches. (Dibeh, Hilal & Charara, 2018) separates maxillary and mandibular jaws using N-degree polynomial regression. (Abdi, Kasaei & Mehdizadeh, 2015) employed a four-step method consists of gap valley extraction, modified canny edge detector, guided iterative contour tracing, and template matching. However, contrasting the overall performance of automated segmentation with individual expert results — all of which were estimated to be above 98%— clearly demonstrates that the computerized process can still be improved to meet the gold standard more precisely.

In (Veena Divya, Jatti & Revan Joshi, 2016), Active contour-based segmentation is proposed for cystic lesion segmentation and extraction to analyze cyst development behavior. The segmentation method has positive results for nonlinear background, poor contrast, and noisy image. (Divya et al., 2019) have compared the level set method and watershed segmentation for the detection of cyst and lesion. The study reveals that the level set segmentation produces more predicted results for cyst/Lesion. An approach used to identify age & gender by analyzing dental images is very useful in the field of biometrics (Avcu & Bacşiftçi, 2020). Several other image processing techniques are used on dental images to achieve the best biometric results. The area of the teeth, the perimeter measure, the center of gravity, the rate of resemblance, and the radius are all used for the estimation of age.

Hybrid Dataset is the image dataset combining different dental imaging modalities used for the analysis. (Said et al., 2006) have used periapical & bitewing X-rays for the teeth segmentation. In this approach, background area is discarded using an appropriate threshold, then mathematical morphology and connected component labeling are applied for the teeth extraction. This approach finds difficulty in extracting images having low contrast between teeth and bones, blurred images, etc. (Tuan, Ngan & others, 2016; Tuan & others, 2017; Tuan et al., 2018) introduced the semi-supervised fuzzy clustering approach with some modification to find the various teeth and bone structures. (Ali, Ejbali & Zaied, 2015) compared CPU & GPU results after applying the chan-Vese model with active contour without edge. It shows that GPU model implementation is several times faster than the CPU version.

Photographic color images are the RGB images of occlusal surfaces that are mainly useful for detecting caries and useful for human identification (Datta & Chaki, 2015a,b). Teeth segmentation is performed by integrating watershed and snake-based techniques on dental RGB images. Subsequently, incisors tooth features extracted for the recognition of a person. Caries identified by applying cluster-based segmentation showing 93% accurate results. This method can segment individual teeth, lesions from caries and track the development of lesion size. This research's primary objective is to find the exact caries lesions of the tooth surfaces, which helps to improve the diagnosis. In (Ghaedi et al., 2014), Caries segmentation employed by using the region-widening method and circular hough transform (CHT), then morphological operations applied to locate the irregular regions around the tooth boundaries. A fully automatic process for the caries classification is given by (Berdouses et al., 2015). Segmentation separates cavitated lesion areas, then after area features extracted to assign the region to a particular class. It can be a valuable method to support the dentist in making a more reliable and accurate analysis of occlusal caries diagnosis.

CT & CBCT Images provide 3D visualization of teeth and help dentists with orthodontic surgery, dental implants, and cosmetic surgeries. (Hoshtalab et al., 2010) suggested a multi-step approach for the teeth classification and numbering in multi-slice CT (MSCT) images. Teeth segmentation is accomplished using otsu's thresholding, morphological operations, panoramic re-sampling, and variational level set. The Wavelet-Fourier descriptor (WFD) with the centroid distance signature is used in a multi-resolution method for feature extraction. Afterward, classification was done using a feed-forward neural network classifier (Hu et al., 2014) compared to otsu's results and mean thresholding using CT images. It shows the results of mean thresholding are better as compare to otsu's based method. A multi-step procedure was introduced by (Mortaheb, Rezaeian & Soltanian-Zadeh, 2013) based on the mean shift algorithm for automatic CT image slices segmentation of the tooth area. (Gao & Li, 2013) grouped data blocks into uniform blocks first, and then an iterative fusion scheme is used to provide the initial labeled and unlabeled events for semi-supervised learning,. (Gao & Chae, 2010) used 18 dental CT image dataset for the segmentation applying active contour tracking algorithms where tracking of the root is done by a single level set method. It shows higher accuracy and visualization of tooth regions as compare to other methods.

2.2 Conventional machine learning algorithms for dental image analysis

Development in the field of Machine Learning (ML) and Artificial Intelligence (AI) is growing over the last few years. ML and AI methods have made a meaningful contribution to the field of dental imaging, such as computer-aided diagnosis & treatment, X-ray image interpretation, image-guided treatment, infected area detection, and information representation adequately and efficiently. The ML and AI make it easier and help doctors diagnose and presume the risk of disease accurately and more quickly in time. Conventional machine learning algorithms for image perception rely exclusively on expertly designed features, i.e., identifying dental caries involves the extraction of texture features—an overview of various machine learning algorithms given in Figure 11.

ML datasets are generally composed of exclusive training, validation, and test sets. It determines system characteristics from the testing data set and validates the features acquired from the evaluation data collection. Using the test dataset, one might finally verify ML's precision and extraction of valuable features to formulate a powerful training model. Table 4 reveals the conventional algorithms' actual results focused on machine learning used for dental image analysis.

2.3 Deep learning techniques for dental image analysis

Artificial Intelligence (AI), machine learning, and deep learning techniques used to assist medical imaging technicians in spotting abnormalities and diagnosing disorders in a fraction of the time required earlier (and with more accurate tests generally). Deep learning is an advancement of artificial neural networks (ANN), which consists of more layers that allow better data predictions (LeCun, Bengio & Hinton, 2015; Schmidhuber, 2015). Deep learning is associated with developing self-learning back-propagation techniques that incrementally optimize data outcomes and computing power increases. The predictive performance of deep learning algorithms in the medical imaging field exceeds human skill levels, transforming the role of computer-assisted diagnosis into a more interactive one (Burt et al., 2018; Park & Park, 2018).

Health diagnostic computer-aided software is used in the medical field as a secondary tool, but developing traditional CAD systems tend to be very strenuous. Recently, there have been introducing deep learning approaches to CAD, with accurate outcomes for different clinical applications (Cheng et al., 2016). The research study mostly used a convolution neural network model to analyze other dental imaging modalities. CNN's are a typical form of deep neural network feed-forward architectures, and they are usually used for computer vision and image object identification tasks. CNN's were initially released about two decades before; however, in 2012, when AlexNet 's architecture significantly outpaced other ImageNet large-scale recognition race challenges (Krizhevsky, Sutskever & Hinton, 2012). Machine vision came in as the deep learning revolution, and since then, CNNs have been rapidly evolving. Feature learning methods have taken a massive turn since the CNN model has come into being that can "learning features" instead of customizing them into the model. Fully convolution neural network using Alexnet, as given in Figure 12, used to categorize teeth, including molar, premolar, canine, and incisor, by training cone-beam CT images (Miki et al., 2017a; Oktay, 2017). (Tuzoff et al., 2019) applied the Faster R-CNN model as given in Figure 13, which interprets pipeline and optimizes computation to detect the tooth (Ren et al., 2017) and VGG-16 convolution architecture for classification (Simonyan & Zisserman, 2014). These methods are beneficial in practical applications and further investigation of computerized dental X-ray image analysis.

In DXRI, CNNs have been extensively used to detect Tooth fractures, bone loss, caries detection, periapical lesions, or also used for the analysis of different dental structures (Lee et al., 2018a; Schwendicke et al., 2019). Neural networks need to be equipped and refined, and a database of dental X-ray images is necessary for that (Lee et al., 2018b). (Lee et al., 2019) applied mask R-CNN model, a multi-tasking model based on a CNN and capable of identifying, classifying, and masking artifacts in an image. A mask R-CNN mask operated in two steps. In the first step, the Region of interest (ROIs) selection procedure was performed. In the second step, the R-CNN mask includes a binary mask similarity to the classification and bounding box foresight for each ROI (Romera-Paredes & Torr, 2016; He et al., 2017).

Dental structures(enamel, dentin, and pulp) identified using U-net architecture show the best outcome (Ronneberger, Fischer & Brox, 2015). CNN is a standard technique for multi-class identification and characterization, but if used explicitly, it requires extensive training to achieve a successful result. In the medical sphere, lack of data is a common problem because of the privacy of people. To address this issue, (Zhang et al., 2018) suggested a technique that uses a label tree to assign multiple labels to each tooth and decompose a task that can manage data shortages. Table 5 shows the results of various deep learning-based techniques in the field of dentistry.

2.4. Performance measures

In general, if the algorithm's efficiency is more significant than other algorithms, one algorithm is prioritized over another. According to a specific domain or research field, various performance measures are used to compare algorithms or machine learning methods. It comprises accuracy, Jaccard index, sensitivity, precision, recall, DSC, F-measure, AUC, MSE, Error rate, etc. The segmentation and classification model output by pointing out the experiment dataset's inaccurate predictions is very significant. Here we include a thorough analysis of the success metrics employed in the field of Dental Image analysis.

2.4.1 Performance metrics used for dental image processing

Calculation of the performance metrics used for dental segmentation is performed by authenticating pixel by pixel and analyzing the segmentation results with the gold standard. Manual segmentation done by a radiologist is considered the gold standard. Pixel-based metrics are measured in terms of accuracy, precision, dice coefficient, specificity, and F-score widely used in segmentation analysis. Some of the problems in analyzing image segmentation are metric selection, the use of multiple meanings for some metrics in the literature, inefficiency of metric measurement implementations that lead to significant large volume dataset difficulties. Poorly described metrics can result in imprecision conclusions on state-of-the-art algorithms, which affects the system's overall growth. Table 6 presents an overview of various metrics widely used by various researchers for dental image segmentation.

The significance of accuracy and assurance is essential in the medical imaging field. Also, the validation of segmentation, therefore, achieves the result and dramatically increases the precision, accuracy, conviction, and computational speed of segmentation. Segmentation methods are especially helpful in computer-aided medical diagnostic applications where the interpretation of objects that are hard to differentiate by human vision is a significant component.

2.4.2 Confusion Matrix

The confusion matrix is used to evaluate the performance of medical image segmentation and classification. The confusion matrix helps identify the relationship between the outcomes of the predictive algorithm and the actual ones. Some of the terms used for the confusion matrix are given in Table 7, True positive (TP): Correctly identified or detected, False positive (FP): Evaluated or observed incorrectly, False negative (FN): wrongly rejected, True Negative (TN): Correctly rejected. In approach (Mahoor & Abdel-Mottaleb, 2005) used two descriptors to identify the molars and premolars. Experimental results show that molars' classification is easier than premolars, and centroid distance is less potent than a complex coordinate signature for teeth classification. The performance of the method suggested by (Nomir & Abdel-Mottaleb, 2007) was evaluated using parameters such as Signature vector, Hierarchical, Force field (FF), and Fourier descriptor (FD). Here, FF & FD give small values for matching Euclidean distance and absolute distance, indicating that the performance is better than the other two methods. (Prajapati, Desai & Modi, 2012) firstly calculates the feature vector of the query image (FVQ) and the feature vector of database images (TnFV) and then evaluate the distance vector (D_n) of the image using the formula: $D_n = \sum |T_n FV - FVQ|$. The minimum value of the distance vector indicates that the best match of the image with the database image.

The method proposed by (Huang et al., 2012) achieved higher isolation accuracy for the upper and lower jaws than the technique given by Nomir and Abdel-Mottaleb. (Harandi & Pourghassem, 2011) proposed a method to evaluate the length of the tooth and compared it with the size estimated by the dentist and then measurement error (ME) is calculated for one canal, two canals, and three canals using the following

$$\text{formula: } ME = \frac{\text{Mesured length}}{\text{Actual length}} .$$

Here measured error is the least for the one canal as compared to the two and three canals. (Niroshika, Meegama & Fernando, 2013) used a standard distance parameter compared with the Kass algorithm. It has been observed that the value of the typical distance parameter is lesser than the Kass algorithm, which means that the suggested method is more useful to trace the boundary of the tooth as compared to the Kass algorithm. (Pushparaj et al., 2013) measured the numbering accuracy (which means whether teeth

are correctly numbered or not) using precision and sensitivity. The numbering performance metric (η) is given by the following equation: $\eta = \frac{(m-n)}{n} * 100$. Where 'm' is total no of teeth numbered and 'n' is erroneously numbered. This approach gives more than 90% accuracy for the numbering of molar and premolars teeth.

In (Abdi, Kasaei & Mehdizadeh, 2015), methods compared the results of mandible segmentation and Hausdorff distance with the manually segmented gold standard. The sensitivity, specificity, and dice similarity coefficient (DSC) are estimated, and the algorithm results seem to be very close to the manually segmented gold standard. (Amer & Aqel, 2015) extract the wisdom teeth and compare the method with the other two approaches by evaluating mean absolute error MAE. The lower value of MAE indicated the best segmentation compared to other methods. In (Poonsri et al., 2016), accuracy is measured using template matching for the single-rooted tooth and double rooted tooth. Here, segmentation accuracy is more than 40%, as mentioned in their research work. (Tuan & others, 2016, 2017) used cluster validity measurement: PBM, Simplified Silhouette Width Criterion (SSWC), Davis-Bouldin (DB), BH, VCR, BR, and TRA, and values of these parameters are indicating best results as compared to the effects of existing algorithms.

PBM: The maximum value of this index is said to be the PBM index, across the hierarchy provides the best partitioning.

Simplified Silhouette Width Criterion (SSWC): The silhouette analysis tests how well the observation is clustered and calculates the average distance between clusters. The silhouette plot shows how similar each point in a cluster is to the neighboring clusters' points.

Davies-Bouldin index (DB): This index determines the average 'similarity' amongst clusters, in which the resemblance is a metric that measures the distance between clusters with the size of clusters themselves. The lower Davies-Bouldin index refers to a model with a greater detachment of clusters.

Ball and Hall index (BH): used to measure the distance within a group, and its higher value indicates better results.

Calinski-Harabasz index, also called Variance Ratio Criterion (VCR): Its higher value is better and is used to calculate the partition data by variance.

Banfeld-Raftery index (BR): It using a variance-covariance matrix of every cluster is measured.

Difference-like index (TRA): used to find the cluster difference, and a larger value is better.

Various Performance measures used in dental X-ray imaging considering deep learning methods are given in figure 14.

2.5. Dataset Description

The researcher in the dental imaging field has used various types of databases. In which some of the databases available online, while some records are not present. The most prominent dilemma is finding out which investigation has given valid results because everyone has shown promising results on their datasets. All the dental imaging databases that have been used so far are mentioned in Table 8.

3. Conclusion

The study addressed various conventional and deep learning techniques applied in the field of dental imaging. It also includes the applications of different imaging modalities in dentistry. The approaches addressed in this article are image processing-based, machine learning, and deep-learning, etc. It is challenging to opt for one type of segmentation technique in conventional image-processing methods

because of various researchers' dataset images' variability. However, the advantage of using traditional methods is the simplicity of implementation and the more inexpensive computing rate. While on the other hand, a variety of CNN architectures have been investigated. Most of the time, individual or personalized networks applied in dental imaging are apparent when most pre-trained networks have not utilized the expected outcome because of the limited amount of data used in most experiments.

The dentists try to analyze the whole dental structure and, if applicable, create the patient's treatment plan using the images acquired with the X-ray. However, due to a shortage of good automated tools to study dental X-ray images, these images are evaluated empirically, that is, solely based on the dentist's knowledge. The challenge of interpreting dental X-rays is better when working with extra-oral images. These images are not restricted to an isolated portion of the teeth, as is in the case with intra-oral X-rays. As we have seen in various works, researchers have used pre-examined images through a manual crop of the area of interest. This procedure makes it hard to correctly interpret and compare outcomes due to small manual procedure mistakes. Many articles have identified networks that have trained to divide images into regions of a particular scale (Lee, Park & Kim, 2017; Rana et al., 2017). While using a similar approach, the network will not learn the entire picture as a whole and focuses only on the small part of the picture. In some papers, the downsampling technique is used because of the limited amount of datasets available, which might delete important details present in the images (Karimian et al., 2018; Wirtz, Mirashi & Wesarg, 2018). It's challenging to validate and verify the algorithm's correctness because of the inadequate datasets available for the hypothesis.

However, the automatic segmentation of DXRI images is a challenging task and has received less attention from the research community.

In this paper, we have presented a comprehensive survey of dental X-ray image segmentation & classification methods for medical diagnosis. Further, we have proposed a novel taxonomy based on the type of dental image used for capturing the teeth structure. Here, we have divided the techniques based on bitewing, periapical, panoramic, CBCT/CT, photographic color images, and hybrid datasets. In the end, comparative analysis in terms of various performance measures is elaborated. It is also observed that in DXRI, there is no standard publicly available data set. In future work, more sophisticated segmentation methods are required for better performance. Another research direction is setting up a DXRI image dataset containing different imaging modalities. In existing DXRI segmentation methods, machine learning has been used up to a limited extent. This stems from another research direction for the future.

References

- Abdi AH, Kasaei S, Mehdizadeh M. 2015. Automatic segmentation of mandible in panoramic x-ray. *Journal of Medical Imaging* 2:44003.
- Abrahams JJ. 2001. Dental CT Imaging: A Look at the Jaw. *Radiology* 219:334–345. DOI: 10.1148/radiology.219.2.r01ma33334.
- Al-sherif N, Guo G, Ammar HH. 2012. A new approach to teeth segmentation. In: *2012 IEEE International Symposium on Multimedia*. 145–148.
- Ali R Ben, Ejbali R, Zaied M. 2015. GPU-based segmentation of dental x-ray images using active contours without edges. In: *2015 15th International Conference on Intelligent Systems Design and Applications (ISDA)*. 505–510.
- Ali M, Khan M, Tung NT, others. 2018. Segmentation of dental X-ray images in medical imaging using

- neutrosophic orthogonal matrices. *Expert Systems with Applications* 91:434–441.
- Aliaga I, Vera V, Vera M, García E, Pedrera M, Pajares G. 2020. Automatic computation of mandibular indices in dental panoramic radiographs for early osteoporosis detection. *Artificial Intelligence in Medicine* 103:101816.
- Alsmadi MK. 2018. A hybrid Fuzzy C-Means and Neutrosophic for jaw lesions segmentation. *Ain Shams Engineering Journal* 9:697–706.
- Amer YY, Aqel MJ. 2015. An efficient segmentation algorithm for panoramic dental images. *Procedia Computer Science* 65:718–725.
- Avuçlu E, Başçıftçi F. 2019. Novel approaches to determine age and gender from dental x-ray images by using multiplayer perceptron neural networks and image processing techniques. *Chaos, Solitons & Fractals* 120:127–138.
- Avuçlu E, Başçıftçi F. 2020. The determination of age and gender by implementing new image processing methods and measurements to dental X-ray images. *Measurement* 149:106985.
- Ayuningtias A, Putra NK, Juliastuti E, Epsilawati L, others. 2013. Quantitative image analysis of periapical dental radiography for dental condition diagnosis. In: *2013 3rd International Conference on Instrumentation, Communications, Information Technology and Biomedical Engineering (ICICI-BME)*. 363–366.
- Banar N, Bertels J, Laurent F, Boedi RM, De Tobel J, Thevissen P, Vandermeulen D. 2020. Towards fully automated third molar development staging in panoramic radiographs. *International Journal of Legal Medicine*:1–11.
- Banday M, Mir AH. 2019. Dental Biometric Identification System using AR Model. In: *TENCON 2019-2019 IEEE Region 10 Conference (TENCON)*. 2363–2369.
- Banu AFS, Kayalvizhi M, Arumugam B, Gurunathan U. 2014. Texture based classification of dental cysts. In: *2014 International Conference on Control, Instrumentation, Communication and Computational Technologies (ICCICCT)*. 1248–1253.
- Benyó B, Szilágyi L, Haidegger T, Kovács L, Nagy-Dobó C. 2009. Detection of the root canal's centerline from dental micro-CT records. In: *2009 Annual International Conference of the IEEE Engineering in Medicine and Biology Society*. 3517–3520.
- Berdouses ED, Koutsouri GD, Tripoliti EE, Matsopoulos GK, Oulis CJ, Fotiadis DI. 2015. A computer-aided automated methodology for the detection and classification of occlusal caries from photographic color images. *Computers in biology and medicine* 62:119–135.
- Black G V. 1981. Extracts from the last century. Susceptibility and immunity by dental caries by G.V. Black. *British dental journal* 151:10. DOI: 10.1038/sj.bdj.4804617.
- Bo C, Liang X, Chu P, Xu J, Wang D, Yang J, Megalooikonomou V, Ling H. 2017. Osteoporosis prescreening using dental panoramic radiographs feature analysis. In: *2017 IEEE 14th International Symposium on Biomedical Imaging (ISBI 2017)*. 188–191.
- Bradley D, Roth G. 2007. Adaptive thresholding using the integral image. *Journal of graphics tools* 12:13–21.
- Burt JR, Torosdagli N, Khosravan N, RaviPrakash H, Mortazi A, Tissavirasingham F, Hussein S, Bagci

- 600 U. 2018. Deep learning beyond cats and dogs: recent advances in diagnosing breast cancer with
601 deep neural networks. *The British journal of radiology* 91:20170545.
- 602 Caruso P, Silvestri E, Sconfienza LM. 2013. *Cone Beam CT and 3D imaging*. Springer Science &
603 Business Media. DOI: 10.1007/978-88-470-5319-9.
- 604 Cheng J-Z, Ni D, Chou Y-H, Qin J, Tiu C-M, Chang Y-C, Huang C-S, Shen D, Chen C-M. 2016.
605 Computer-aided diagnosis with deep learning architecture: applications to breast lesions in US
606 images and pulmonary nodules in CT scans. *Scientific reports* 6:1–13.
- 607 Choi J, Eun H, Kim C. 2018. Boosting proximal dental caries detection via combination of variational
608 methods and convolutional neural network. *Journal of Signal Processing Systems* 90:87–97.
- 609 Chu P, Bo C, Liang X, Yang J, Megalooikonomou V, Yang F, Huang B, Li X, Ling H. 2018. Using
610 octuplet siamese network for osteoporosis analysis on dental panoramic radiographs. In: *2018 40th*
611 *Annual International Conference of the IEEE Engineering in Medicine and Biology Society*
612 *(EMBC)*. 2579–2582.
- 613 Datta S, Chaki N. 2015a. Person identification technique using RGB based dental images. In: *IFIP*
614 *International Conference on Computer Information Systems and Industrial Management*. 169–180.
- 615 Datta S, Chaki N. 2015b. Detection of dental caries lesion at early stage based on image analysis
616 technique. In: *2015 IEEE International Conference on Computer Graphics, Vision and Information*
617 *Security (CGVIS)*. 89–93.
- 618 Datta S, Chaki N, Modak B. 2019. A Novel Technique to Detect Caries Lesion Using Isophote Concepts.
619 *IRBM* 40:174–182.
- 620 Datta S, Chaki N, Modak B. 2020. Neutrosophic Set-Based Caries Lesion Detection Method to Avoid
621 Perception Error. *SN Computer Science* 1:63.
- 622 Devi RK, Banumathi A, Ulaganathan G. 2019. An automated and hybrid method for cyst segmentation in
623 dental X-ray images. *Cluster Computing* 22:12179–12191.
- 624 Dibeh G, Hilal A, Charara J. 2018. A Novel Approach for Dental Panoramic Radiograph Segmentation.
625 In: *2018 IEEE International Multidisciplinary Conference on Engineering Technology (IMCET)*. 1–
626 6.
- 627 Divya KV, Jatti A, Joshi PR, Krishna SD. 2019. A Correlative Study of Contrary Image Segmentation
628 Methods Appending Dental Panoramic X-ray Images to Detect Jawbone Disorders. In: *Progress in*
629 *Advanced Computing and Intelligent Engineering*. Springer, 25–35.
- 630 Dykstra B. 2008. Interproximal caries detection: how good are we? *Dentistry today* 27:144–146.
- 631 Egger J, Pfarrkirchner B, Gsaxner C, Lindner L, Schmalstieg D, Wallner J. 2018. Fully convolutional
632 mandible segmentation on a valid ground-truth dataset. In: *2018 40th Annual International*
633 *Conference of the IEEE Engineering in Medicine and Biology Society (EMBC)*. 656–660.
- 634 Eun H, Kim C. 2016. Oriented tooth localization for periapical dental X-ray images via convolutional
635 neural network. In: *2016 Asia-Pacific Signal and Information Processing Association Annual*
636 *Summit and Conference (APSIPA)*. 1–7.
- 637 Fariza A, Arifin AZ, Astuti ER, Kurita T. 2019. Segmenting tooth components in dental X-ray images
638 using Gaussian kernel- based conditional spatial Fuzzy C-Means clustering algorithm. *International*

- 639 *Journal of Intelligent Engineering and Systems* 12. DOI: 10.22266/IJIES2019.0630.12.
- 640 Fernandez K, Chang C. 2012. Teeth/palate and interdental segmentation using artificial neural networks.
641 In: *IAPR Workshop on Artificial Neural Networks in Pattern Recognition*. 175–185.
- 642 Frejlichowski D, Wanat R. 2011. Automatic segmentation of digital orthopantomograms for forensic
643 human identification. In: *International Conference on Image Analysis and Processing*. 294–302.
- 644 Fukuda M, Inamoto K, Shibata N, Arijji Y, Yanashita Y, Kutsuna S, Nakata K, Katsumata A, Fujita H,
645 Arijji E. 2019. Evaluation of an artificial intelligence system for detecting vertical root fracture on
646 panoramic radiography. *Oral Radiology*:1–7.
- 647 Gao H, Chae O. 2008. Automatic tooth region separation for dental CT images. In: *2008 Third*
648 *International Conference on Convergence and Hybrid Information Technology*. 897–901.
- 649 Gao H, Chae O. 2010. Individual tooth segmentation from CT images using level set method with shape
650 and intensity prior. *Pattern Recognition* 43:2406–2417.
- 651 Gao Y, Li X. 2013. Teeth segmentation via semi-supervised learning. In: *2013 6th International*
652 *Conference on Biomedical Engineering and Informatics*. 558–563.
- 653 Geetha V, Aprameya KS, Hinduja DM. 2020. Dental caries diagnosis in digital radiographs using back-
654 propagation neural network. *Health Information Science and Systems* 8:1–14.
- 655 Ghaedi L, Gottlieb R, Sarrett DC, Ismail A, Belle A, Najarian K, Hargraves RH. 2014. An automated
656 dental caries detection and scoring system for optical images of tooth occlusal surface. In: *2014 36th*
657 *Annual International Conference of the IEEE Engineering in Medicine and Biology Society*. 1925–
658 1928.
- 659 Goyal B, Agrawal S, Sohi BS. 2018. Noise Issues Prevailing in Various Types of Medical Images.
660 *Biomedical & Pharmacology Journal* 11:1227.
- 661 Harandi AA, Pourghassem H. 2011. A semi automatic algorithm based on morphology features for
662 measuring of root canal length. In: *2011 IEEE 3rd International Conference on Communication*
663 *Software and Networks*. 260–264.
- 664 Harandi AA, Pourghassem H, Mahmoodian H. 2011. Upper and lower jaw segmentation in dental X-ray
665 image using modified active contour. In: *2011 international conference on intelligent computation*
666 *and bio-medical instrumentation*. 124–127.
- 667 Hatvani J, Horváth A, Michetti J, Basarab A, Kouamé D, Gyöngy M. 2018. Deep learning-based super-
668 resolution applied to dental computed tomography. *IEEE Transactions on Radiation and Plasma*
669 *Medical Sciences* 3:120–128.
- 670 He K, Gkioxari G, Dollár P, Girshick R. 2017. Mask r-cnn. In: *Proceedings of the IEEE international*
671 *conference on computer vision*. 2961–2969.
- 672 Hiraiwa T, Arijji Y, Fukuda M, Kise Y, Nakata K, Katsumata A, Fujita H, Arijji E. 2019. A deep-learning
673 artificial intelligence system for assessment of root morphology of the mandibular first molar on
674 panoramic radiography. *Dentomaxillofacial Radiology* 48:20180218.
- 675 Hosntalab M, Zoroofi RA, Tehrani-Fard AA, Shirani G. 2010. Classification and numbering of teeth in
676 multi-slice CT images using wavelet-Fourier descriptor. *International journal of computer assisted*
677 *radiology and surgery* 5:237–249.

- 678 Hossain MF, Alsharif MR, Yamashita K. 2010. Medical image enhancement based on nonlinear
679 technique and logarithmic transform coefficient histogram matching. In: *IEEE/ICME International*
680 *Conference on Complex Medical Engineering*. 58–62.
- 681 Hu Z, Wu PZ, Gui J, Chen Y, Zheng H. 2014. Teeth segmentation using dental CT data. In: *2014 7th*
682 *International Conference on Biomedical Engineering and Informatics*. 81–84.
- 683 Huang C-H, Hsu C-Y. 2008. Computer-assisted orientation of dental periapical radiographs to the
684 occlusal plane. *Oral Surgery, Oral Medicine, Oral Pathology, Oral Radiology, and Endodontology*
685 105:649–653.
- 686 Huang P-W, Lin P-L, Kuo C-H, Cho YS. 2012. An effective tooth isolation method for bitewing dental
687 X-ray images. In: *2012 International Conference on Machine Learning and Cybernetics*. 1814–
688 1820.
- 689 Iannucci J, Howerton LJ. 2012. *Dental Radiography, 5th Edition*. Elsevier saunders.
- 690 Imangaliyev S, van der Veen MH, Volgenant CMC, Keijser BJF, Crielaard W, Levin E. 2016. Deep
691 learning for classification of dental plaque images. In: *International Workshop on Machine*
692 *Learning, Optimization, and Big Data*. 407–410.
- 693 Jader G, Fontineli J, Ruiz M, Abdalla K, Pithon M, Oliveira L. 2018. Deep instance segmentation of teeth
694 in panoramic X-ray images. In: *2018 31st SIBGRAPI Conference on Graphics, Patterns and Images*
695 *(SIBGRAPI)*. 400–407.
- 696 Jain KR, Chauhan NC. 2017. An Automatic Segmentation Approach Towards the Objectification of Cyst
697 Diagnosis in Periapical Dental Radiograph. In: *International Conference on Information and*
698 *Communication Technology for Intelligent Systems*. 164–172.
- 699 Ji DX, Ong SH, Foong KWC. 2014. A level-set based approach for anterior teeth segmentation in cone
700 beam computed tomography images. *Computers in biology and medicine* 50:116–128.
- 701 Karimian N, Salehi HS, Mahdian M, Alnajjar H, Tadinada A. 2018. Deep learning classifier with optical
702 coherence tomography images for early dental caries detection. In: *Lasers in Dentistry XXIV*.
703 1047304.
- 704 Kats L, Vered M, Zlotogorski-Hurvitz A, Harpaz I. 2019. Atherosclerotic carotid plaque on panoramic
705 radiographs: neural network detection. *Int J Comput Dent* 22:163–169.
- 706 Kim J, Lee H-S, Song I-S, Jung K-H. 2019. DeNTNet: Deep Neural Transfer Network for the detection of
707 periodontal bone loss using panoramic dental radiographs. *Scientific reports* 9:1–9.
- 708 Krizhevsky A, Sutskever I, Hinton GE. 2012. Imagenet classification with deep convolutional neural
709 networks. In: *Advances in neural information processing systems*. 1097–1105.
- 710 Kumar A, Bhadauria HS, Singh A. 2020. Semi-supervised OTSU based hyperbolic tangent Gaussian
711 kernel fuzzy C-mean clustering for dental radiographs segmentation. *Multimedia Tools and*
712 *Applications* 79:2745–2768.
- 713 Kushol R, Raihan M, Salekin MS, Rahman ABM, others. 2019. Contrast Enhancement of Medical X-Ray
714 Image Using Morphological Operators with Optimal Structuring Element. *arXiv preprint*
715 *arXiv:1905.08545*.
- 716 Kutsch VK. 2011. Caries Detection, Inside Dentistry. *AEGIS Communications*.

- 717 Lai YH, Lin PL. 2008. Effective segmentation for dental X-ray images using texture-based fuzzy
718 inference system. In: *International Conference on Advanced Concepts for Intelligent Vision*
719 *Systems*. 936–947.
- 720 LeCun Y, Bengio Y, Hinton G. 2015. Deep learning. *nature* 521.
- 721 Lee J-H, Han S-S, Kim YH, Lee C, Kim I. 2019. Application of a fully deep convolutional neural
722 network to the automation of tooth segmentation on panoramic radiographs. *Oral Surgery, Oral*
723 *Medicine, Oral Pathology and Oral Radiology*.
- 724 Lee J-H, Kim D, Jeong S-N, Choi S-H. 2018a. Diagnosis and prediction of periodontally compromised
725 teeth using a deep learning-based convolutional neural network algorithm. *Journal of periodontal &*
726 *implant science* 48:114–123.
- 727 Lee J-H, Kim D-H, Jeong S-N, Choi S-H. 2018b. Detection and diagnosis of dental caries using a deep
728 learning-based convolutional neural network algorithm. *Journal of dentistry* 77:106–111.
- 729 Lee H, Park M, Kim J. 2017. Cephalometric landmark detection in dental x-ray images using
730 convolutional neural networks. In: *Medical Imaging 2017: Computer-Aided Diagnosis*. 101341W.
- 731 Li X, Abaza A, Nassar DE, Ammar H. 2006. Fast and accurate segmentation of dental x-ray records. In:
732 *International Conference on Biometrics*. 688–696.
- 733 Li S, Fevens T, Krzyżak A, Jin C, Li S. 2005. Toward automatic computer aided dental X-ray analysis
734 using level set method. In: *International Conference on Medical Image Computing and Computer-*
735 *Assisted Intervention*. 670–678.
- 736 Li S, Fevens T, Krzyżak A, Jin C, Li S. 2007. Semi-automatic computer aided lesion detection in dental
737 X-rays using variational level set. *Pattern Recognition* 40:2861–2873.
- 738 Lin P-L, Huang P-Y, Huang P-W. 2012. An automatic lesion detection method for dental X-ray images
739 by segmentation using variational level set. In: *2012 International Conference on Machine Learning*
740 *and Cybernetics*. 1821–1825.
- 741 Lin PL, Huang PY, Huang PW, Hsu HC, Chen CC. 2014. Teeth segmentation of dental periapical
742 radiographs based on local singularity analysis. *Computer methods and programs in biomedicine*
743 113:433–445.
- 744 Lira PHM, Giraldo GA, Neves LAP, Feijoo RA. 2014. Dental r-ray image segmentation using texture
745 recognition. *IEEE Latin America Transactions* 12:694–698.
- 746 Mahdi FP, Kobashi S. 2018. Quantum Particle Swarm Optimization for Multilevel Thresholding-Based
747 Image Segmentation on Dental X-Ray Images. In: *2018 Joint 10th International Conference on Soft*
748 *Computing and Intelligent Systems (SCIS) and 19th International Symposium on Advanced*
749 *Intelligent Systems (ISIS)*. 1148–1153.
- 750 Mahoor MH, Abdel-Mottaleb M. 2004. Automatic classification of teeth in bitewing dental images. In:
751 *2004 International Conference on Image Processing, 2004. ICIIP'04*. 3475–3478.
- 752 Mahoor MH, Abdel-Mottaleb M. 2005. Classification and numbering of teeth in dental bitewing images.
753 *Pattern Recognition* 38:577–586. DOI: 10.1016/j.patcog.2004.08.012.
- 754 Mendonça EA. 2004. Clinical decision support systems: perspectives in dentistry. *Journal of dental*
755 *education* 68:589–597.

- Menon HP, Rajeshwari B. 2016. Enhancement of dental digital X-ray images based on the image quality. In: *The International Symposium on Intelligent Systems Technologies and Applications*. 33–45.
- Miki Y, Muramatsu C, Hayashi T, Zhou X, Hara T, Katsumata A, Fujita H. 2017a. Classification of teeth in cone-beam CT using deep convolutional neural network. *Computers in biology and medicine* 80:24–29.
- Miki Y, Muramatsu C, Hayashi T, Zhou X, Hara T, Katsumata A, Fujita H. 2017b. Tooth labeling in cone-beam CT using deep convolutional neural network for forensic identification. In: *Medical Imaging 2017: Computer-Aided Diagnosis*. 101343E.
- Molteni R. 1993. Direct digital dental x-ray imaging with Visualix/VIXA. *Oral surgery, oral medicine, oral pathology* 76:235–243.
- Mortaheb P, Rezaeian M, Soltanian-Zadeh H. 2013. Automatic dental CT image segmentation using mean shift algorithm. In: *2013 8th Iranian Conference on Machine Vision and Image Processing (MVIP)*. 121–126.
- Muramatsu C, Morishita T, Takahashi R, Hayashi T, Nishiyama W, Arijji Y, Zhou X, Hara T, Katsumata A, Arijji E, others. 2020. Tooth detection and classification on panoramic radiographs for automatic dental chart filing: improved classification by multi-sized input data. *Oral Radiology*:1–7.
- Murata M, Arijji Y, Ohashi Y, Kawai T, Fukuda M, Funakoshi T, Kise Y, Nozawa M, Katsumata A, Fujita H, others. 2019. Deep-learning classification using convolutional neural network for evaluation of maxillary sinusitis on panoramic radiography. *Oral radiology* 35:301–307.
- Nassar DEM, Ammar HH. 2007. A neural network system for matching dental radiographs. *Pattern Recognition* 40:65–79.
- Niroshika UAA, Meegama RGN, Fernando TGI. 2013. Active contour model to extract boundaries of teeth in dental X-ray images. In: *2013 8th International Conference on Computer Science & Education*. 396–401.
- Nomir O, Abdel-Mottaleb M. 2005. A system for human identification from X-ray dental radiographs. *Pattern Recognition* 38:1295–1305.
- Nomir O, Abdel-Mottaleb M. 2007. Human identification from dental X-ray images based on the shape and appearance of the teeth. *IEEE transactions on information forensics and security* 2:188–197.
- Nomir O, Abdel-Mottaleb M. 2008. Fusion of matching algorithms for human identification using dental X-ray radiographs. *IEEE Transactions on Information Forensics and Security* 3:223–233.
- Nuansanong J, Kiattisin S, Leelasantitham A. 2014. Diagnosis and interpretation of dental X-ray in case of deciduous tooth extraction decision in children using active contour model and J48 tree. In: *2014 International Electrical Engineering Congress (iEECON)*. 1–4.
- Obuchowicz Rafałand Nurzynska K, Obuchowicz B, Urbanik A, Piórkowski A. 2018. *Caries detection enhancement using texture feature maps of intraoral radiographs*.
- Oktay AB. 2017. Tooth detection with Convolutional Neural Networks. In: *2017 Medical Technologies National Congress (TIPTKNO)*. 1–4.
- Olsen GF, Brilliant SS, Primeaux D, Najarian K. 2009. An image-processing enabled dental caries detection system. In: *2009 ICME International Conference on Complex Medical Engineering*. 1–8.

- 795 Oprea S, Marinescu C, Lita I, Jurianu M, Visan DA, Cioc IB. 2008. Image processing techniques used for
796 dental x-ray image analysis. In: *2008 31st international spring seminar on electronics technology*.
797 125–129.
- 798 Osterloh D, Viriri S. 2019. Caries Detection in Non-standardized Periapical Dental X-Rays. In: *Computer*
799 *Aided Intervention and Diagnostics in Clinical and Medical Images*. Springer, 143–152.
- 800 Park WJ, Park J-B. 2018. History and application of artificial neural networks in dentistry. *European*
801 *journal of dentistry* 12:594–601.
- 802 Patanachai N, Covavisaruch N, Sinthanayothin C. 2010. Wavelet transformation for dental X-ray
803 radiographs segmentation technique. In: *2010 Eighth International Conference on ICT and*
804 *Knowledge Engineering*. 103–106.
- 805 Poonsri A, Aimjirakul N, Charoenpong T, Sukjamsri C. 2016. Teeth segmentation from dental x-ray
806 image by template matching. In: *2016 9th Biomedical Engineering International Conference*
807 *(BMEiCON)*. 1–4.
- 808 Prajapati DB, Desai NP, Modi CK. 2012. A simple and novel CBIR technique for features extraction
809 using AM dental radiographs. In: *2012 International Conference on Communication Systems and*
810 *Network Technologies*. 198–202.
- 811 Prajapati SA, Nagaraj R, Mitra S. 2017. Classification of dental diseases using CNN and transfer
812 learning. In: *2017 5th International Symposium on Computational and Business Intelligence*
813 *(ISCBI)*. 70–74.
- 814 Prakash M, Gowsika U, Sathiyapriya S. 2015. An identification of abnormalities in dental with support
815 vector machine using image processing. In: *Emerging Research in Computing, Information,*
816 *Communication and Applications*. Springer, 29–40.
- 817 Purnama IKE, Kurniastuti I, Rinastiti M, Purnomo MH. 2015. Semi-automatic determination of root
818 canal length in dental X-ray image. In: *2015 4th International Conference on Instrumentation,*
819 *Communications, Information Technology, and Biomedical Engineering (ICICI-BME)*. 49–53.
- 820 Pushparaj V, Gurunathan U, Arumugam B. 2013. An effective dental shape extraction algorithm using
821 contour information and matching by mahalanobis distance. *Journal of digital imaging* 26:259–268.
- 822 Pushparaj V, Gurunathan U, Arumugam B, Baskaran A, Valliappan A. 2013. An effective numbering and
823 classification system for dental panoramic radiographs. In: *2013 Fourth International Conference*
824 *on Computing, Communications and Networking Technologies (ICCCNT)*. 1–8.
- 825 Rad AE, Amin IBM, Rahim MSM, Kolivand H. 2015. Computer-aided dental caries detection system
826 from X-ray images. In: *Computational Intelligence in Information Systems*. Springer, 233–243.
- 827 Rad AE, Mohd Rahim MS, Rehman A, Altameem A, Saba T. 2013. Evaluation of current dental
828 radiographs segmentation approaches in computer-aided applications. *IETE Technical Review*
829 30:210–222.
- 830 Rad AE, Rahim MSM, Kolivand H, Norouzi A. 2018. Automatic computer-aided caries detection from
831 dental x-ray images using intelligent level set. *Multimedia Tools and Applications* 77:28843–28862.
- 832 Ramani R, Vanitha NS, Valarmathy S. 2013. The pre-processing techniques for breast cancer detection in
833 mammography images. *International Journal of Image, Graphics and Signal Processing* 5:47.

- 834 Rana A, Yaune G, Wong LC, Gupta O, Muftu A, Shah P. 2017. Automated segmentation of gingival
835 diseases from oral images. In: *2017 IEEE Healthcare Innovations and Point of Care Technologies*
836 *(HI-POCT)*. 144–147.
- 837 Razali MRM, Ahmad NS, Hassan R, Zaki ZM, Ismail W. 2014. Sobel and canny edges segmentations for
838 the dental age assessment. In: *2014 International Conference on Computer Assisted System in*
839 *Health*. 62–66.
- 840 Razifar P, Sandström M, Schnieder H, Långström B, Maripuu E, Bengtsson E, Bergström M. 2005. Noise
841 correlation in PET, CT, SPECT and PET/CT data evaluated using autocorrelation function: a
842 phantom study on data, reconstructed using FBP and OSEM. *BMC medical imaging* 5:5.
- 843 Ren S, He K, Girshick R, Sun J. 2017. Faster r-cnn: Towards real-time object detection with region
844 proposal networks In *IEEE Transactions on Pattern Analysis and Machine Intelligence* (pp. 1137--
845 1149). *Los Alamitos, CA: IEEE* 10.
- 846 Romera-Paredes B, Torr PHS. 2016. Recurrent instance segmentation. In: *European conference on*
847 *computer vision*. 312–329.
- 848 Ronneberger O, Fischer P, Brox T. 2015. U-net: Convolutional networks for biomedical image
849 segmentation. In: *International Conference on Medical image computing and computer-assisted*
850 *intervention*. 234–241.
- 851 Said E, Fahmy GF, Nassar D, Ammar H. 2004. Dental x-ray image segmentation. In: *Biometric*
852 *Technology for Human Identification*. 409–417.
- 853 Said EH, Nassar DEM, Fahmy G, Ammar HH. 2006. Teeth segmentation in digitized dental X-ray films
854 using mathematical morphology. *IEEE transactions on information forensics and security* 1:178–
855 189.
- 856 Sarage GN, Jambhorkar S. 2012. Enhancement of chest X-ray images using filtering techniques. *Int J Adv*
857 *Res Comput Sci Softw Eng* 2:308–312.
- 858 Sattar F, Karray FO. 2012. Dental x-ray image segmentation and object detection based on phase
859 congruency. In: *International Conference Image Analysis and Recognition*. 172–179.
- 860 Schmidhuber J. 2015. Deep learning in neural networks: An overview. *Neural networks* 61:85–117.
- 861 Schwendicke F, Golla T, Dreher M, Krois J. 2019. Convolutional neural networks for dental image
862 diagnostics: A scoping review. *Journal of dentistry*:103226.
- 863 Shah S, Abaza A, Ross A, Ammar H. 2006. Automatic tooth segmentation using active contour without
864 edges. In: *2006 Biometrics Symposium: Special Session on Research at the Biometric Consortium*
865 *Conference*. 1–6.
- 866 Sharma M, Rana NK, Kundra H. 2015. A Review on the Existing Image Segmentation Techniques for the
867 Dental X-Ray Images. 3:15–19.
- 868 Silva G, Oliveira L, Pithon M. 2018. Automatic segmenting teeth in X-ray images: Trends, a novel data
869 set, benchmarking and future perspectives. *Expert Systems with Applications* 107:15–31.
- 870 Simonyan K, Zisserman A. 2014. Very deep convolutional networks for large-scale image recognition.
871 *arXiv preprint arXiv:1409.1556*.

- 872 Singh HV, Agarwal R. 2018. Diagnosis of Carious Lesions Using Digital Processing of Dental
873 Radiographs. In: *Computational Vision and Bio Inspired Computing*. Springer, 864–882.
- 874 Singh P, Sehgal P. 2020. Numbering and Classification of Panoramic Dental Images Using 6-Layer
875 Convolutional Neural Network. *Pattern Recognition and Image Analysis* 30:125–133.
- 876 Sornam M, Prabhakaran M. 2017. A new linear adaptive swarm intelligence approach using back
877 propagation neural network for dental caries classification. In: *2017 IEEE International Conference*
878 *on Power, Control, Signals and Instrumentation Engineering (ICPCSI)*. 2698–2703.
- 879 Srivastava MM, Kumar P, Pradhan L, Varadarajan S. 2017. Detection of tooth caries in bitewing
880 radiographs using deep learning. *arXiv preprint arXiv:1711.07312*.
- 881 Subramanyam RB, Prasad KP, Anuradha B. 2014. Different Image Segmentation Techniques for Dental
882 Image Extraction. *Int. Journal of Engineering Research and Applications* 4:173–177.
- 883 Torosdagli N, Liberton DK, Verma P, Sincan M, Lee JS, Bagci U. 2018. Deep geodesic learning for
884 segmentation and anatomical landmarking. *IEEE transactions on medical imaging* 38:919–931.
- 885 Tracy KD, Dykstra BA, Gakenheimer DC, Scheetz JP, Lacina S, Scarfe WC, Farman AG. 2011. Utility
886 and effectiveness of computer-aided diagnosis of dental caries. *Gen Dent* 59:136–144.
- 887 Tuan TM, Fujita H, Dey N, Ashour AS, Ngoc VTN, Chu D-T, others. 2018. Dental diagnosis from X-ray
888 images: an expert system based on fuzzy computing. *Biomedical Signal Processing and Control*
889 39:64–73.
- 890 Tuan TM, Ngan TT, others. 2016. A novel semi-supervised fuzzy clustering method based on interactive
891 fuzzy satisficing for dental X-ray image segmentation. *Applied Intelligence* 45:402–428.
- 892 Tuan TM, others. 2016. A cooperative semi-supervised fuzzy clustering framework for dental X-ray
893 image segmentation. *Expert Systems with Applications* 46:380–393.
- 894 Tuan TM, others. 2017. Dental segmentation from X-ray images using semi-supervised fuzzy clustering
895 with spatial constraints. *Engineering Applications of Artificial Intelligence* 59:186–195.
- 896 Tuzoff D V, Tuzova LN, Bornstein MM, Krasnov AS, Kharchenko MA, Nikolenko SI, Sveshnikov MM,
897 Bednenko GB. 2019. Tooth detection and numbering in panoramic radiographs using convolutional
898 neural networks. *Dentomaxillofacial Radiology* 48:20180051.
- 899 Valizadeh S, Goodini M, Ehsani S, Mohseni H, Azimi F, Bakhshandeh H. 2015. Designing of a computer
900 software for detection of approximal caries in posterior teeth. *Iranian Journal of Radiology* 12.
- 901 Veena Divya K, Jatti A, Revan Joshi P. 2016. Appending active contour model on digital panoramic
902 dental X-rays images for segmentation of maxillofacial region. In: *2016 IEEE EMBS Conference on*
903 *Biomedical Engineering and Sciences (IECBES), Kaula Lumpur, Malaysia*. 4–8.
- 904 Vijayakumari B, Ulaganathan G, Banumathi A, Banu AFS, Kayalvizhi M. 2012. Dental cyst diagnosis
905 using texture analysis. In: *2012 International Conference on Machine Vision and Image Processing*
906 *(MVIP)*. 117–120.
- 907 Vila-Blanco N, Tomás I, Carreira MJ. 2018. Fully Automatic Teeth Segmentation in Adult OPG Images.
908 *Multidisciplinary Digital Publishing Institute Proceedings* 2:1199.
- 909 Wang C-W, Huang C-T, Lee J-H, Li C-H, Chang S-W, Siao M-J, Lai T-M, Ibragimov B, Vrtovec T,

- 910 Ronneberger O, others. 2016. A benchmark for comparison of dental radiography analysis
911 algorithms. *Medical image analysis* 31:63–76.
- 912 Wirtz A, Mirashi SG, Wesarg S. 2018. Automatic teeth segmentation in panoramic X-ray images using a
913 coupled shape model in combination with a neural network. In: *International Conference on*
914 *Medical Image Computing and Computer-Assisted Intervention*. 712–719.
- 915 Wolff MS, Allen K, Kaim J. 2007. A 100-year journey from GV Black to minimal surgical intervention.
916 *Compendium of continuing education in dentistry (Jamesburg, NJ: 1995)* 28:130–4.
- 917 Yang J, Xie Y, Liu L, Xia B, Cao Z, Guo C. 2018. Automated dental image analysis by deep learning on
918 small dataset. In: *2018 IEEE 42nd Annual Computer Software and Applications Conference*
919 *(COMPSAC)*. 492–497.
- 920 Yilmaz E, Kayikcioglu T, Kayipmaz S. 2017. Computer-aided diagnosis of periapical cyst and
921 keratocystic odontogenic tumor on cone beam computed tomography. *Computer methods and*
922 *programs in biomedicine* 146:91–100.
- 923 Zak J, Korzynska A, Roszkowiak L, Siemion K, Walerzak S, Walerzak M, Walerzak K. 2017. The
924 method of teeth region detection in panoramic dental radiographs. In: *International Conference on*
925 *Computer Recognition Systems*. 298–307.
- 926 Zhang K, Wu J, Chen H, Lyu P. 2018. An effective teeth recognition method using label tree with
927 cascade network structure. *Computerized Medical Imaging and Graphics* 68:61–70.
- 928 Zhou J, Abdel-Mottaleb M. 2005. A content-based system for human identification based on bitewing
929 dental X-ray images. *Pattern Recognition* 38:2132–2142.
- 930

Figure 1

Selected benchmarks for different years for dental imaging methods

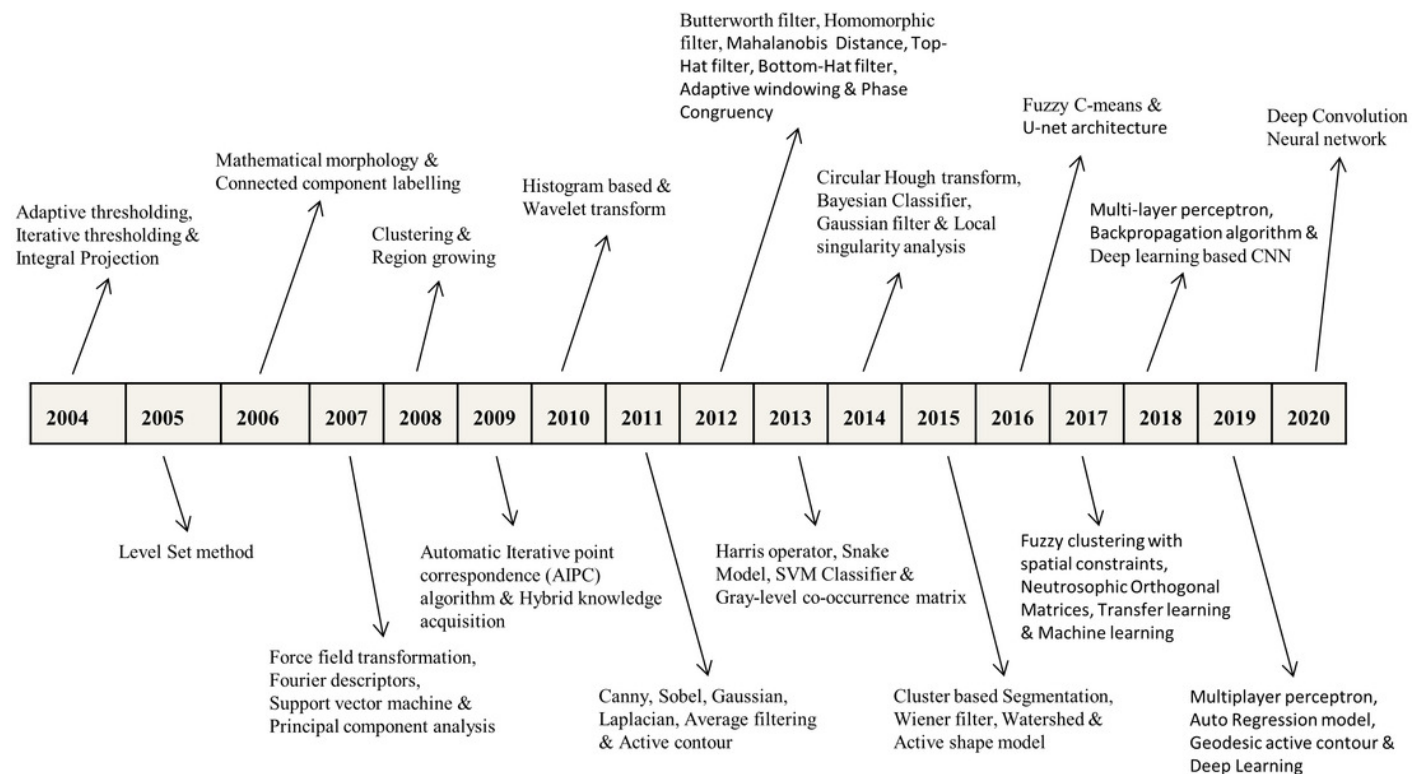


Figure 2

Overview of dental imaging modalities

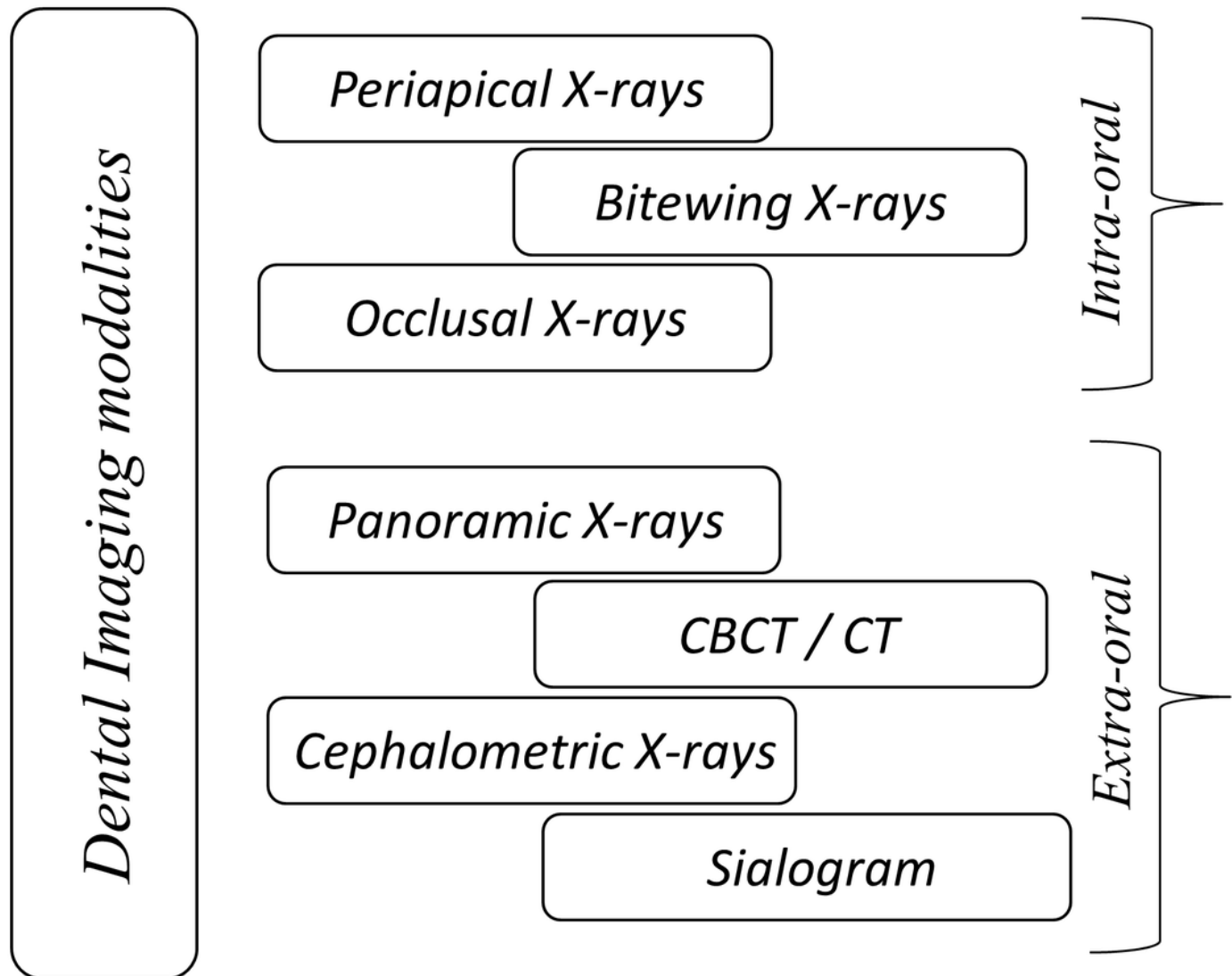


Figure 3

Caries Classification (Black, 1981; Wolff, Allen & Kaim, 2007)

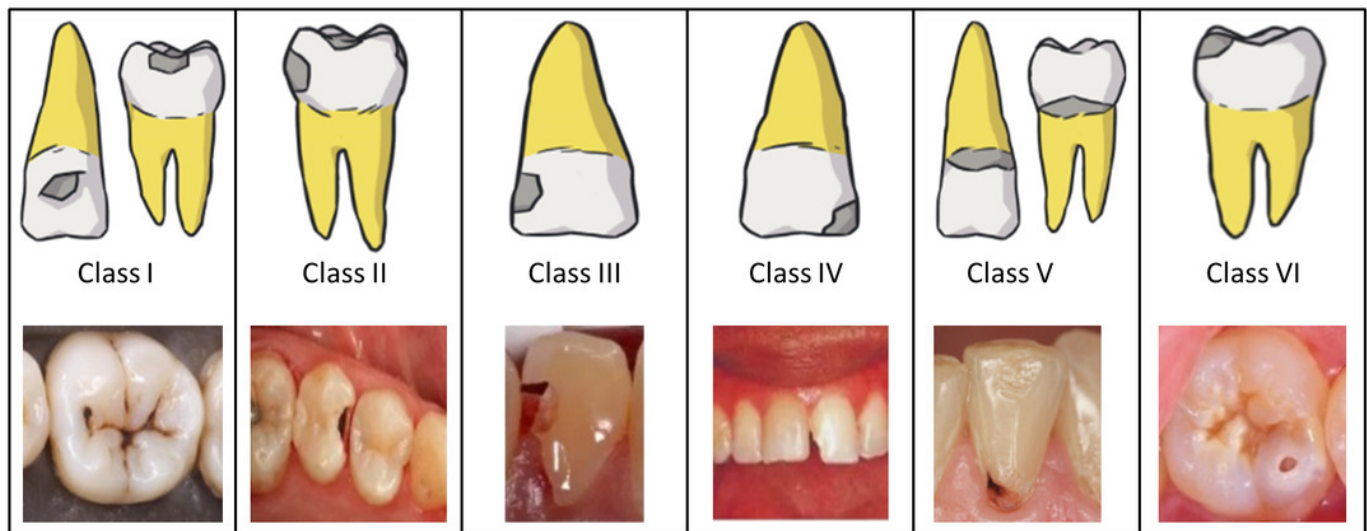


Figure 4

Caries Classification (Iannucci & Howerton, 2012)

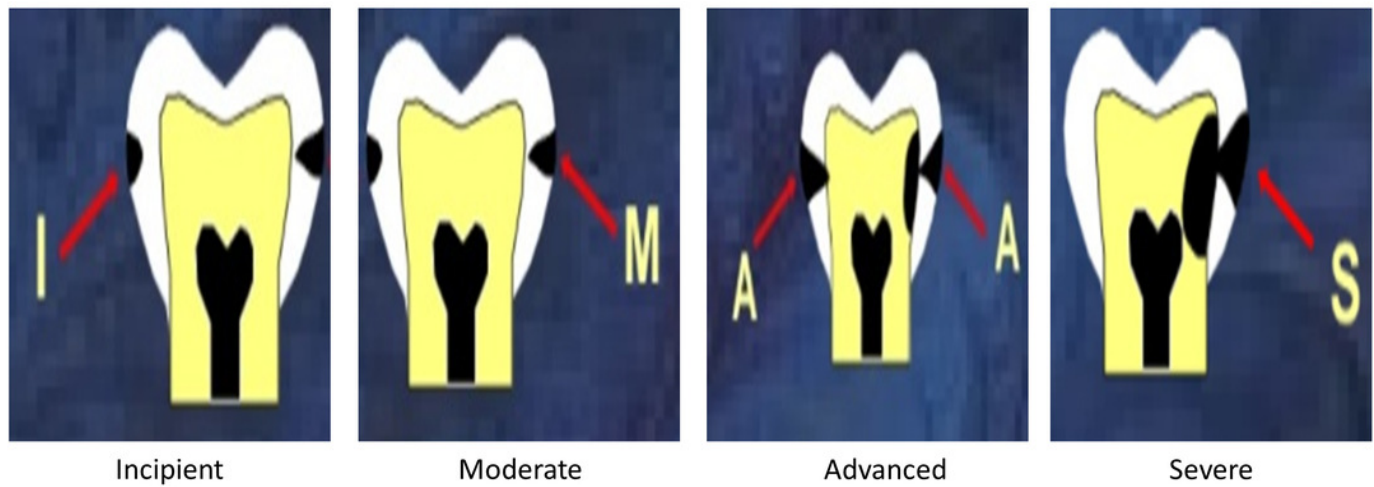


Figure 5

(a) Caries affected (b) Interproximal caries (c) Restoration completed (d) Missing tooth

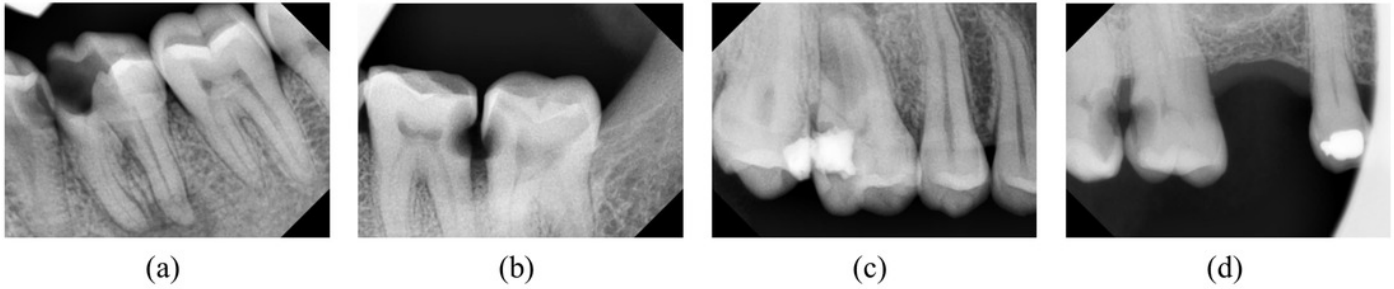


Figure 6

(a) Before RCT. (b) After RCT. (c) Tooth under RCT (d) Final restoration not done.

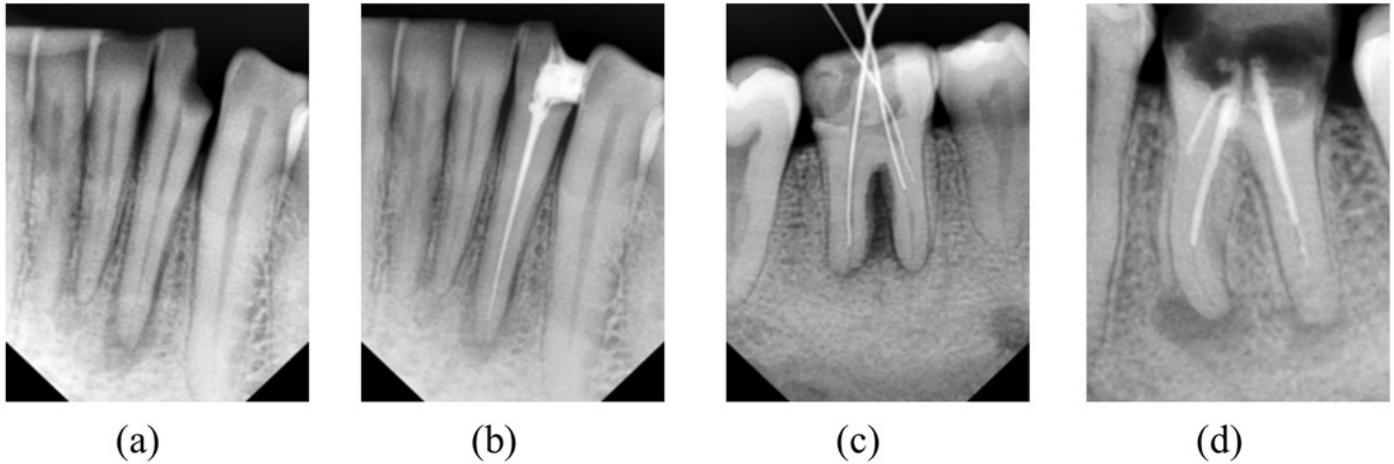


Figure 7

Proposed taxonomy of DXRI methods

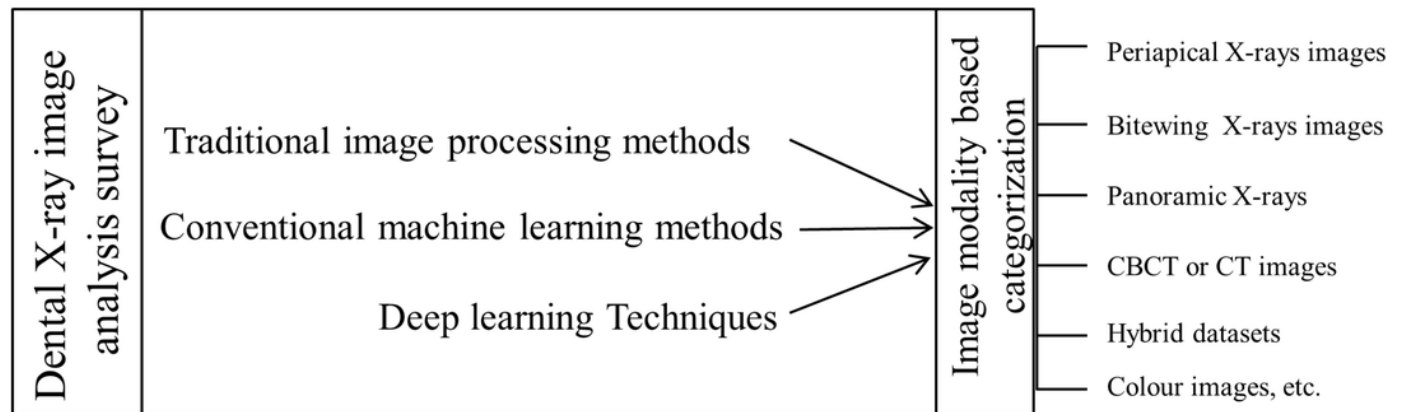


Figure 8

Number of research articles as per publication years in DXRI

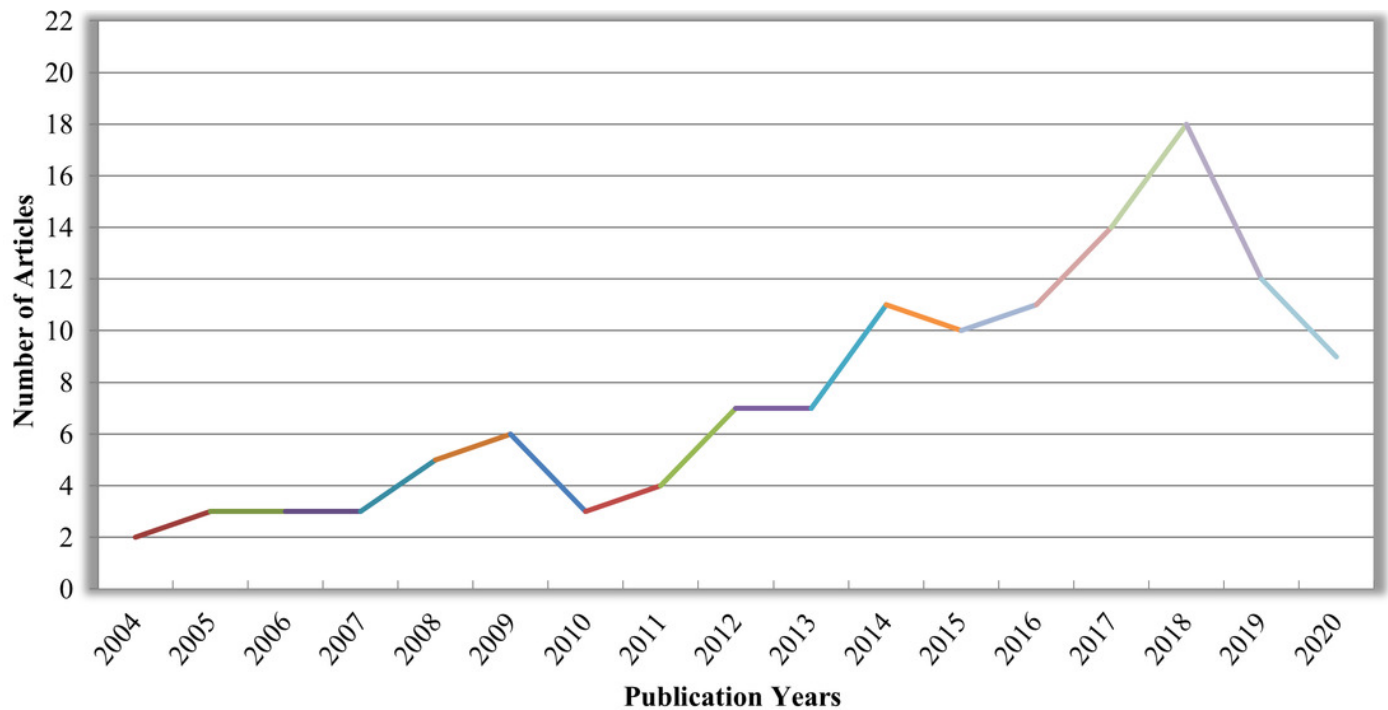


Figure 9

Traditional model used for dental image segmentation and classification

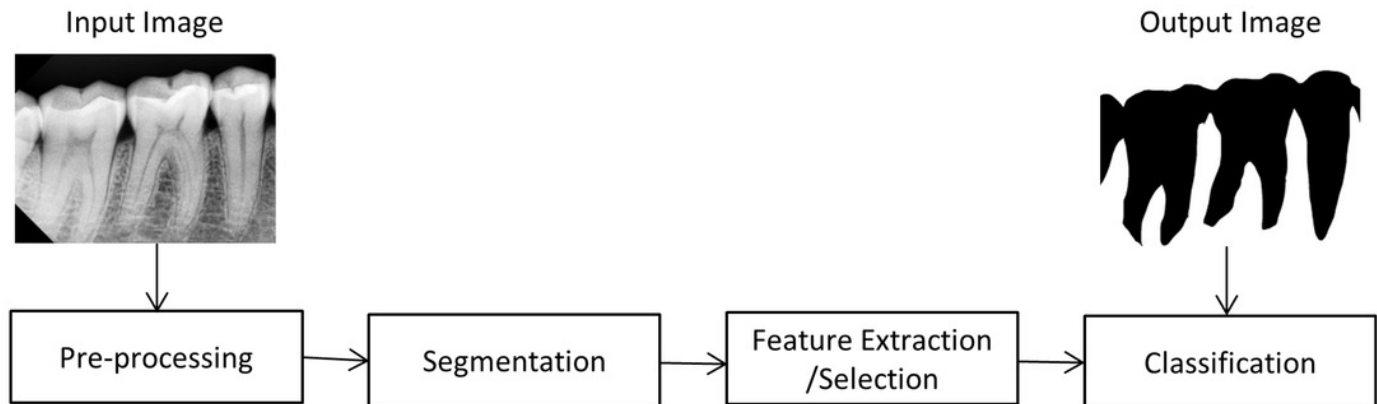


Figure 10

Purpose of Segmentation & problems in dental imaging

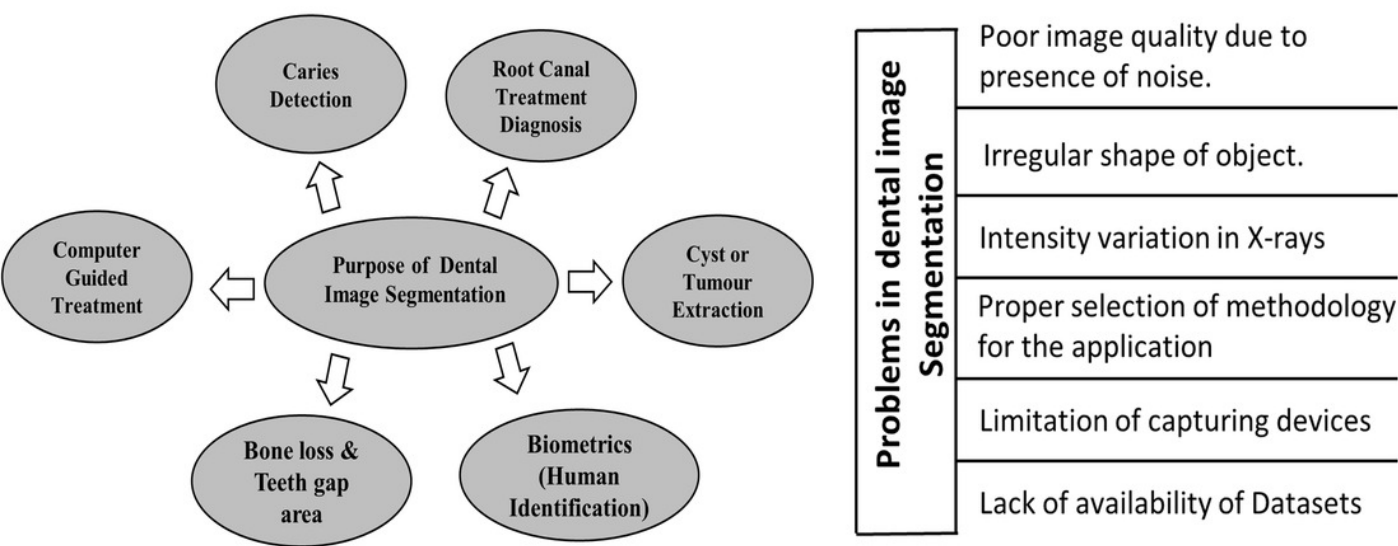


Figure 11

Overview of machine learning algorithms

Machine Learning Algorithms		
Supervised learning		Unsupervised learning
Classification	Regression	Clustering
<ul style="list-style-type: none"> Support Vector Machines (SVM) Discriminant Analysis Naïve Bayes Nearest Neighbour 	<ul style="list-style-type: none"> Linear Regression Non-Linear Regression Decision Trees Neural Networks Ensemble Methods 	<ul style="list-style-type: none"> K-Means, Fuzzy C-means Non-Linear Regression Hierarchical Neural Networks Ensemble Methods Gaussian Mixture Hidden Markov Model

Figure 12

AlexNet architecture for dental images (Miki et al., 2017a,b)

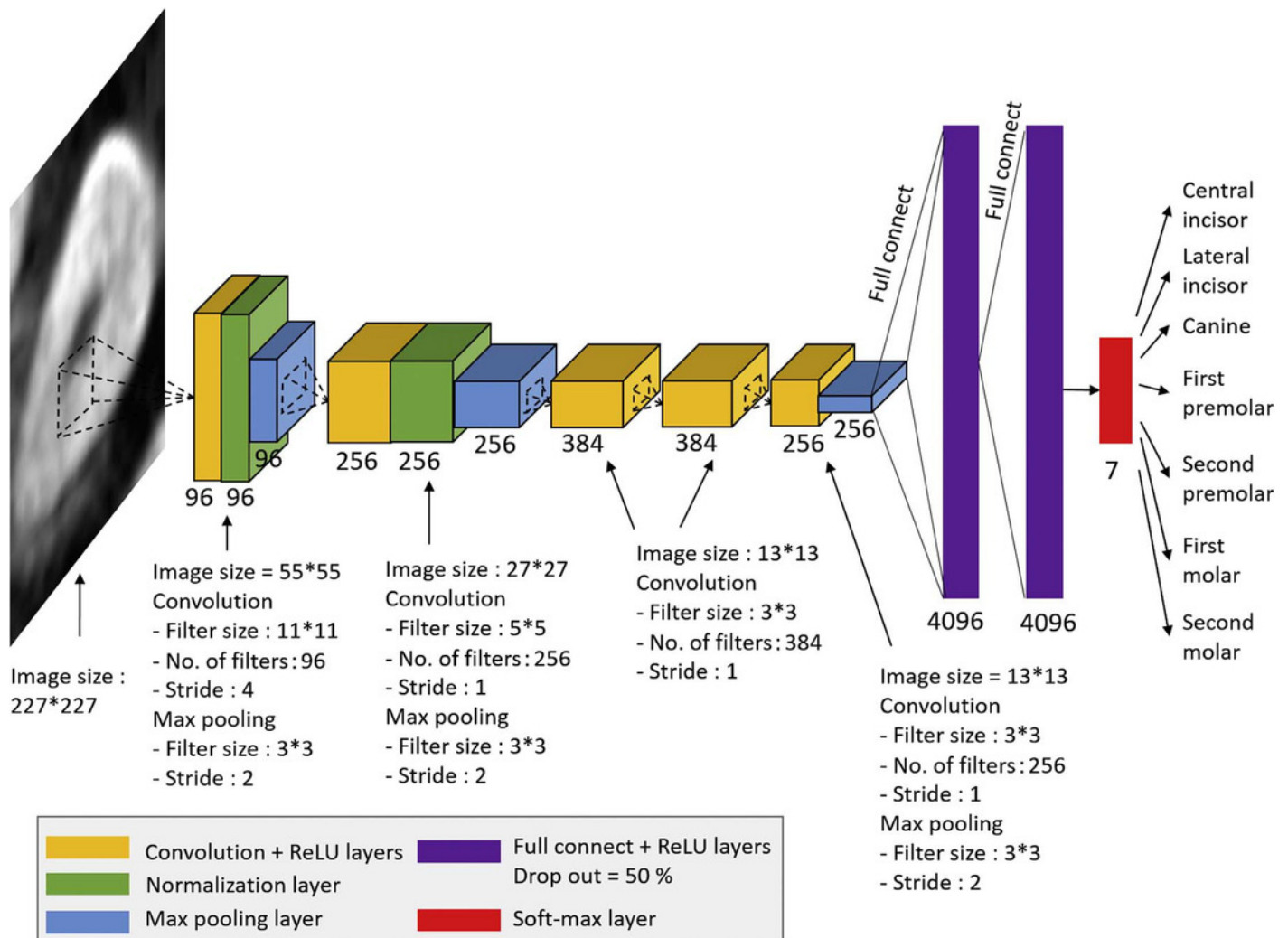


Figure 13

Teeth detection and classification architecture using CNN (Tuzoff et al., 2019)

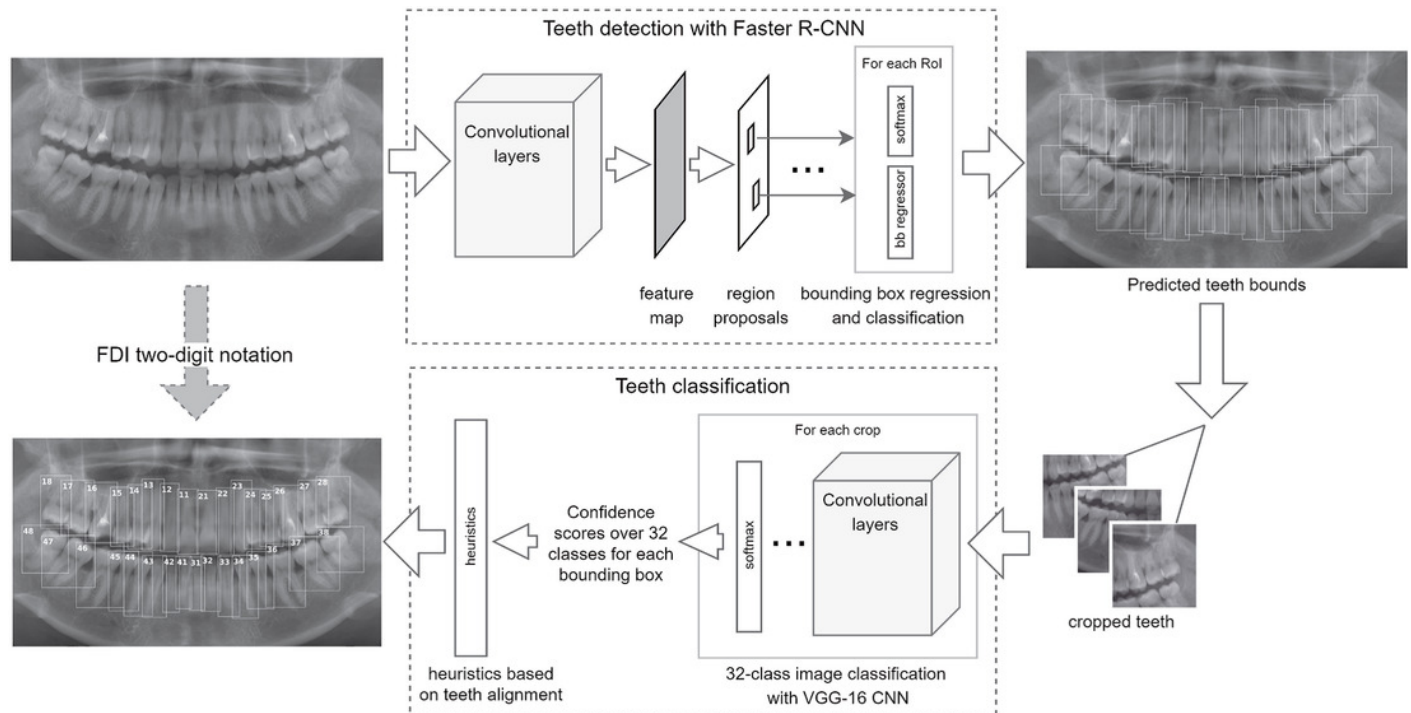
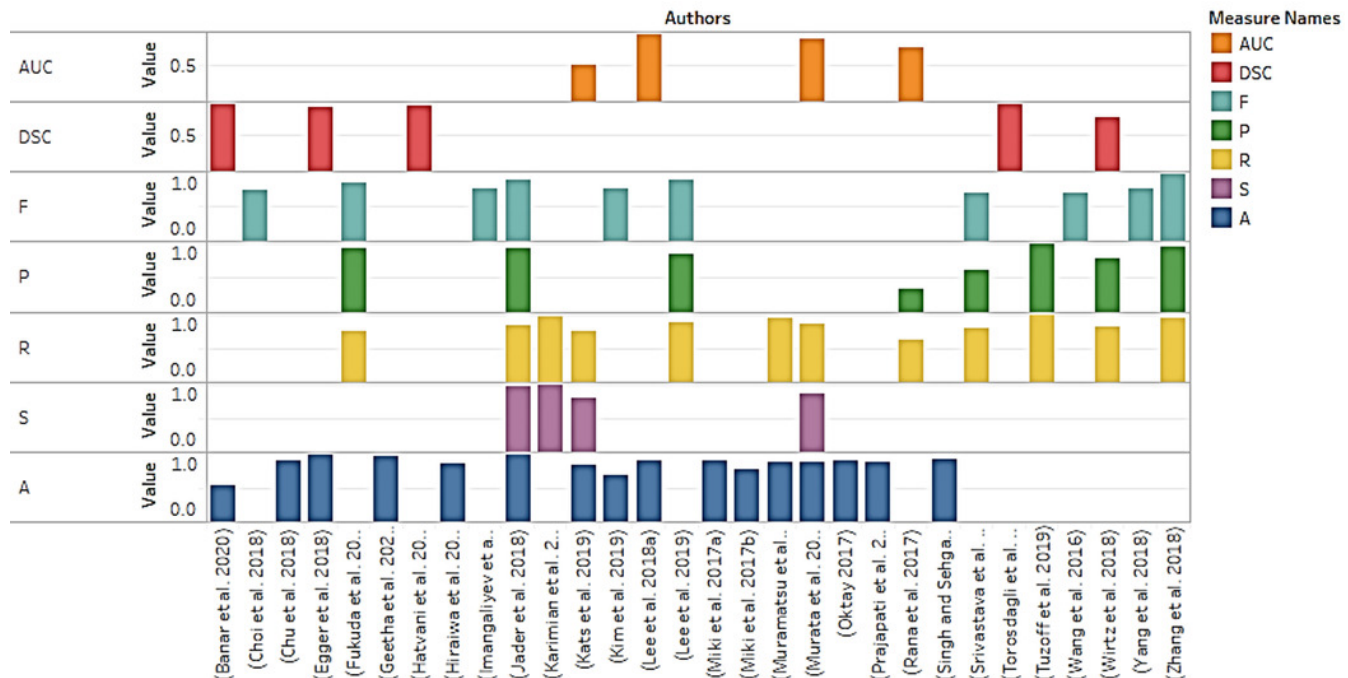


Figure 14

Performances measure comparisons used for deep learning methods

Comparison of Performance Measures



A, AUC, DSC, F, P, R and S for each Authors. Colour shows details about A, AUC, DSC, F, P, R and S.

Table 1 (on next page)

Number of articles categorized based on imaging modalities

Table 1 Number of articles categorized based on imaging modalities

Image modalities	Number of articles published
Periapical X-ray images	30
Bitewing X-ray images	11
Panoramic X-ray images	39
CBCT or CT images	13
Photographic Color Images	06
Hybrid Dataset	19
Image dataset not defined	07

Table 2 (on next page)

Pre-processing methods used for dental imaging modality

Table 1 Pre-processing methods used for dental imaging modality

Author & Year	Enhancement / Noise removal Technique
Methods used for Bitewing X-ray	
(Lai & Lin, 2008)	Adaptive Local Contrast Stretching is used to make the tooth region smoother after that, and adaptive morphological enhancement is applied to improve the texture values.
(Prajapati, Desai & Modi, 2012)	A median filter is used to eradicate picture impulse noise.
(Mahoor & Abdel-Mottaleb, 2004; Zhou & Abdel-Mottaleb, 2005; Huang et al., 2012)	Top hat and bottom hat filters are applied where the teeth become brightened, and the bone and shadow regions obscured.
(Pushparaj, Gurunathan & Arumugam, 2013)	Butterworth high pass filter used with a homomorphic filter. In which homomorphic filter compensates the effect of non-uniform illumination.
Methods used for Periapical X-ray	
(Harandi & Pourghassem, 2011)	Histogram equalization and noise reduction with wavelets, use of spatial filters like Laplacian filter.
(Lin, Huang & Huang, 2012)	Average filter with 25*25 mask then histogram equalization is used.
(Nuansanong, Kiattisin & Leelasantham, 2014)	Gaussian spatial filter with kernel size 5*5 and sigma value 1.4 is fixed.
(Lin et al., 2014)	Enhancement is done by combining adaptive power law transformation, local singularity, and bilateral filter.
(Rad et al., 2015)	Median filtering is applied to enhance the images
(Purnama et al., 2015)	Contrast stretching used to improve the X-ray quality so that it can be easily interpreted and examined correctly
(Jain & Chauhan, 2017)	Gaussian filtering employed to make a more smoothed gradient nearby the edges also helps in reducing noise.
(Obuchowicz Rafał and Nurzyńska et al., 2018)	Histogram equalization (HEQ) and a statistical dominance algorithm (SDA) are initiated.
(Singh & Agarwal, 2018)	Median filtering is used to lower noise, and an unsharp marking filter is used to enhance the high-frequency component.
(Datta, Chaki & Modak, 2019)	Local averaging is used to eliminate noisy features.
(Kumar, Bhadauria & Singh, 2020)	The guided filter is applied with a window size of 3 *3 and is cast-off towards calculating output pixel size.
Methods used for Panoramic X-rays	
(Frejlichowski & Wanat, 2011)	Some basic filters are added to select pyramid layers, including sharpening filter and contrast adjustment before image recomposition.
(Vijayakumari et al., 2012)	Block analysis and contrast stretching applied.
(Pushparaj et al., 2013)	In this paper, the integration of the Butterworth bandpass filter and the homomorphic filter is used to enhance the edges and illumination.
(Razali et al., 2014)	Canny edge detection is applied, where the gaussian filter is used to eliminate the noise.
(Banu et al., 2014)	Image inverse and contrast stretching procedures have been used to identify the region of interest.
(Amer & Aqel, 2015)	Contrast enhancement with intensity transformations is used to improve the segmentation procedure.
(Poonsri et al., 2016)	Image enhancement using adaptive thresholding (Bradley & Roth, 2007).
(Veena Divya, Jatti & Revan Joshi, 2016)	The image contrast is balanced to enhance the picture's appearance and to visualize the cyst or tumor.
(Zak et al., 2017)	A combination of top hat/bottom hat filter and adaptive power-law transformation(APLT) is used to enhance images.
(Alsmadi, 2018)	Speckle noise is reduced by using a median filter.
(Divya et al., 2019)	Negative transformation applied and caries identified by using the difference of contrast improved Image and image negative.
(Banday & Mir, 2019)	Adaptive histogram equalization (CLAHE) and Median Filtering are combinedly applied.
(Fariza et al., 2019)	Dental X-ray image is processed using CLAHE, and gamma correction is done to improve the contrast.
(Ayuçlu & Bacsıftçı, 2020)	Median softening filter applied after contrast stretching.
Methods used for Hybrid Dataset	
(Said et al., 2006)	Internal noise is reduced by closing top-hat transformation, which is described by subtracting the picture from its morphological closure.
(Tuan, Ngan & others, 2016)	Background noise is minimized using a Gaussian filter; then, a Gaussian(DoG) filter is used to measure the gradient along the x and y-axis.
Methods used for Color Images	

(Ghaedi et al., 2014)	A contrast enhancement focused on the histogram is introduced to the gray-level Image.
(Datta & Chaki, 2015a)	Denoising is done by using a wiener filter.
(Datta & Chaki, 2015b)	A Wiener filter is applied to eliminate the blurring effect and additive noise.
(Berdouses et al., 2015)	Gray level transformation performed.
Methods used for CBCT & CT	
(Benyó et al., 2009)	Image with high-frequency noise are enhanced by applying a median filter
(Ji, Ong & Foong, 2014)	Initially, the Intensity range was adjusted, followed by Gaussian filtering with a standard deviation to suppress noise.

Table 3(on next page)

The table shows relevant review findings of the image processing techniques using different imaging modalities

Table 1 The table shows relevant review findings of the image processing techniques using different imaging modalities

Author & Year	Relevant review findings	Total images	Detection/Identification
Imaging modality: Bitewing X-rays			
(Mahoor & Abdel-Mottaleb, 2004)	For Segmentation, adaptive thresholding methods is being used, then features are extracted, and teeth numbering is done using the Bayesian classification technique.	50	Teeth numbering
(Zhou & Abdel-Mottaleb, 2005)	Proposed Segmentation using a window-based adaptive thresholding scheme and minimum Hausdorff distance used for matching purposes	Training =102 images Testing=40 images	Human identification
(Nomir & Abdel-Mottaleb, 2005)	Results are improved by using a signature vector in conjunction with adaptive and iterative thresholding.	117	Human identification
(Nomir & Abdel-Mottaleb, 2007)	Iterative followed by adaptive thresholding used for the Segmentation and features extracted using fourier descriptors after forcefield transformation then matching is done by using euclidian distance	162	Human identification
(Lai & Lin, 2008)	The B-spline curve is used to extract intensity and texture characteristics for K-means clustering to locate the bones and teeth contour.	N.A	Teeth detection
(Nomir & Abdel-Mottaleb, 2008)	The procedure starts with an iterative process guided by adaptive thresholding. Finally, the Bayesian framework is employed for tooth matching.	187	Human identification
(Harandi, Pourghassem & Mahmoodian, 2011)	An active geodesic contour is employed for upper and lower jaws segmentation.	14	Jaw identification
(Huang et al., 2012)	An adaptive windowing scheme with isolation-curve verification is used to detect missing tooth regions.	60	Missing teeth detection
(Prajapati, Desai & Modi, 2012)	A region growing technique is applied to the X-rays to extract the tooth; then, the content-based image retrieval (CBIR) technique is used for matching purposes.	30	Human identification
(Pushparaj, Gurunathan & Arumugam, 2013)	The tooth area's shape is extracted using contour-based connected component labeling, and the Mahalanobis distance (MD) is measured for matching.	50	Person identification
Imaging modality: Periapical X-rays			
(Huang & Hsu, 2008)	Binary image transformations, thresholding, quartering, characterization, and labeling were all used as part of the process.	420	Teeth detection
(Oprea et al., 2008)	Simple thresholding technique applied for Segmentation of caries.	N.A	Caries detection
(Harandi & Pourghassem, 2011)	Otsu thresholding method with canny edge detection is used to segment the root canal area.	43	Root canal detection
(Lin, Huang & Huang, 2012)	The lesion is detected using a variational level set method after applying otsu's method.	6	Lesion detection
(Sattar & Karray, 2012)	Phase congruency based approach is used to provide a framework for local image structure + edge detection	N.A	Teeth detection
(Niroshika, Meegama & Fernando, 2013)	Deformation and re-parameterize are added to the contour to detect the tooth corner points.	N.A	Teeth detection
(Ayuningtiyas et al., 2013)	Dentin and pulp are separated using active contour, and qualitative analysis is conducted using the dentist's visual inspection, while quantitative testing is done by measuring different statistic parameters.	N.A	Tooth detection
(Nuansanong, Kiattisin & Leelasantham, 2014)	Canny edge detection was initially used, followed by an active contour model with data mining (J48 tree) and integration with the competence path.	Approx. 50	Tooth detection
(Lin et al., 2014)	The otsu's threshold and connected component analysis are used to precisely segment the teeth from alveolar bones and remove false teeth areas.	28	Teeth detection
(Purnama et al., 2015)	For root canal segmentation, an active shape model and thinning (using a hit-and-miss transform) were used.	7	Root canal detection
(Rad et al., 2015)	The Segmentation is initially done using K-means clustering. Then, using a gray-level co-occurrence matrix, characteristics were extracted from the X-rays.	32	Caries detection
(Jain & Chauhan, 2017)	First, all parameter values defined in the snake model then initial contour points initializes, and at last canny edge detection extract the	N.A	Cyst detection

	affected part.		
(Singh & Agarwal, 2018)	The color to mark the carious lesion is provided by the contrast limited adaptive histogram (CLAHE) technique combined with masking.	23	Caries detection
(Rad et al., 2018)	The level set segmentation process (LS) is used in two stages. The first stage is the initial contour creation to create the most appropriate IC, and the second stage is the artificial neural network-based smart level approach.	120	Caries detection
(Obuchowicz Rafal and Nurzynska et al., 2018)	K-means clustering applied considering intensity values and first-order features (FOF) detect the caries spots	10	Caries detection
(Devi, Banumathi & Ulaganathan, 2019)	The hybrid algorithm is applied using isophote curvature and the fast marching method (FMM) to extract the cyst.	3	Cyst detection
(Datta, Chaki & Modak, 2019)	The geodesic active contour method is applied to identify the dental caries lesion.	120	Caries detection
(Osterloh & Viriri, 2019)	Proposed unsupervised model to extract the caries region. Jaws partition is done using thresholding and an integral projection algorithm. The top and bottom hats, as well as active contours, were used to detect caries borders.	N.A	Caries detection
(Kumar, Bhadauria & Singh, 2020)	The various dental structures were separated using the fuzzy C-means algorithm and the hyperbolic tangent gaussian kernel function.	152	Dental structures
(Datta, Chaki & Modak, 2020)	This method converts the X-ray image data into its neutrosophic analog domain. A custom feature called 'weight' is used for neutrosophication. Contrary to popular belief, this feature is determined by merging other features.	120	Caries detection
Imaging Modality: Panoramic X-rays			
(Patanachai, Covavisaruch & Sinthanayothin, 2010)	The wavelet transform, thresholding segmentation, and adaptive thresholding segmentation are all compared. Where, the results of wavelet transform show better accuracy as compare to others.	N.A	Teeth detection
(Frejlichowski & Wanat, 2011)	An automatic human identification system applies a horizontal integral projection to segment the individual tooth in this approach.	218	Human identification
(Vijayakumari et al., 2012)	A gray level co-occurrence matrix is used to detect the cyst (GLCM).	3	Cyst detection
(Pushparaj et al., 2013)	Horizontal integral projection with a B-spline curve is employed to separate maxilla and mandible	N.A	Teeth numbering
(Lira et al., 2014)	Supervised learning used for segmentation and feature extraction is carried out through computing moments and statistical characteristics. At last, the bayesian classifier is used to identify different classes.	1	Teeth detection
(Banu et al., 2014)	The gray level co-occurrence matrix is used to compute texture characteristics (GLCM) and classification results obtained in the feature space, focusing on the centroid and K-mean classifier.	23	Cyst detection
(Razali et al., 2014)	This study aims to compare the edge segmentation methods: Canny and Sobel on X-ray images.	N.A	Teeth detection
(Amer & Aqel, 2015)	The segmentation process uses the global Ots's thresholding technique with linked component labeling. The ROI extraction and post-processing are completed at the end.	1	Wisdom teeth detection
(Abdi, Kasaei & Mehdizadeh, 2015)	Four stages used for Segmentation: Gap valley extraction, canny edge with morphological operators, contour tracing, and template matching.	95	Mandible detection
(Veena Divya, Jatti & Revan Joshi, 2016)	Active contour or snake model used to detect the cyst boundary.	10	Cyst detection
(Poonsri et al., 2016)	Teeth identification, template matching using correlation, and area segmentation using K-means clustering are used.	25	Teeth detection
(Zak et al., 2017)	Individual arc teeth segmentation (IATS) with adaptive thresholding is applied to find the palatal bone.	94	Teeth detection
(Alsmadi, 2018)	In panoramic X-ray images that can help in diagnosing jaw lesions, the fuzzy C-means concept and the neutrosophic technique are combinedly used to segment jaw pictures and locate the jaw lesion region.	60	Lesion detection
(Dibeh, Hilal & Charara, 2018)	The methods use a shape-free layout fitted into a 9-degree polynomial curve to segment the area between the maxillary and mandibular jaws.	62	Jaw separation+teeth detection

(Mahdi & Kobashi, 2018)	Quantum Particle Swarm Optimization (QPSO) is employed for multilevel thresholding.	12	Teeth detection
(Ali et al., 2018)	A new clustering method based on the neutrosophic orthogonal matrix is presented to help in the extraction of teeth and jaws areas from panoramic X-rays.	66	Teeth detection
(Divya et al., 2019)	Textural details extracted using GLCM to classify the cyst and caries.	10	Dental caries & cyst extraction
(Bandy & Mir, 2019)	Edge detection method for the Segmentation then, the Autoregression(AR) model is adopted, and AR coefficients are derived from the feature vector. At last, matching is performed using euclidean distance.	210	Human identification
(Fariza et al., 2019)	For tooth segmentation, the Gaussian kernel-based conditional spatial fuzzy c-means (GK-csFCM) clustering algorithm is used.	10	Teeth detection
(Aliaga et al., 2020)	The region of interest is extracted from the entire X-ray image, and Segmentation is performed using k-means clustering.	370	Osteoporosis detection, mandible detection
(Avcu & Bacstiftci, 2020)	The Image is converted to binary using Otsu's thresholding, and then a canny edge detector is used to find the object of interest.	1315	Determination of age and gender
Imaging modality: Hybrid dataset images			
(Said et al., 2006)	Thresholding with mathematical morphology is performed for the Segmentation.	500 Bitewing & 130 Periapical images.	Teeth detection
(Li et al., 2006)	The fast and accurate segmentation approach used strongly focused on mathematical morphology and shape analysis.	500 (Bitewing and Periapical images)	Person identification
(Al-sharif, Guo & Ammar, 2012)	A two-phase threshold processing is used, starting with an iterative threshold followed by an adaptive threshold to binarize teeth images after separating the individual tooth using the seam carving method.	500 Bitewing & 130 Periapical images	Teeth detection
(Ali, Ejbaei & Zaied, 2015)	The Chan-veese model and an active contour without edges are used to divide an image into two regions with piece-constant intensities.	N.A	Teeth detection
(Tuan & others, 2016)	The otsu threshold procedure, fuzzy C-means, and semi-supervised fuzzy clustering are all part of a collaborative framework (eSFCM).	8 & 56 Image dataset (Bitewing+Panoramic)	Teeth structures
(Tuan, Ngan & others, 2016)	It uses a semi-supervised fuzzy clustering algorithm – SSFC-FS based on the Interactive Fuzzy Satisficing method.	56 (Periapical & Panoramic)	Teeth structures
(Tuan & others, 2017)	Semi-supervised fuzzy clustering algorithm combined with spatial constraints (SSFC-SC) for dental image segmentation.	56 (Periapical & panoramic images)	Teeth structures
(Tuan et al., 2018)	Graph-based clustering algorithm called enhanced affinity propagation clustering (APC) used for classification process and fuzzy aggregation operators used for disease detection.	87 (Periapical & Panoramic)	Disease detection
Imaging modality: Photographic color images			
(Ghaedi et al., 2014)	Segmentation functions in two ways. In the first step, the tooth surface is partitioned using a region-widening approach and the Circular Hough Transform (CHT). The second stage uses morphology operators to quantify texture to define the abnormal areas of the tooth's boundaries. Finally, a random forest classifies the various classes.	88	Caries detection
(Datta & Chaki, 2015a)	They have proposed a biometrics dental technique using RGB images. Segment individual teeth with water Shed and Snake's help, then afterward incisors teeth features are obtained to identify the human.	270 Images dataset	Person identification
(Datta & Chaki, 2015b)	The proposed method introduces a method for filtering optical teeth images and extracting caries lesions followed by cluster-based Segmentation.	45	Caries detection
(Berdouses et al., 2015)	The proposed scheme included two processes: (a) identification, in which regions of interest (pre-cavitated and cavitated occlusal lesions) were partitioned, and (b) classification, in which the identified zones were categorized into one of the seven ICDAS classes.	103	Caries detection
Imaging modality: CT & CBCT			
(Gao & Chae, 2008)	The multi-step procedure using thresholding, dilation, connected component labeling, upper-lower jaw separation, and last arch curve fitting was used to find the tooth region.	N.A	Teeth detection
(Hosntalab et al.,	Otsu thresholding, morphological operations, And panoramic re-	30 Multislice	Teeth detection and

2010)	sampling, and variational level set were used. Following that, feature extraction with a wavelet-Fourier descriptor (WFD) and a centroid distance signature is accomplished. Finally, multilayer perceptron (MLP), Kohonen self-organizing network, and hybrid structure are used for Classification.	CT image (MSCT) dataset consists of 804 teeth	Classification
(Gao & Chae, 2010)	An adaptive active contour tracking algorithm is used. In which the root is tracked using a single level set technique. In addition, the variational level was increased in several ways.	18 CT images	Teeth detection
(Mortaeheb, Rezaeian & Soltanian-Zadeh, 2013)	Mean shift algorithm is used for CBCT segmentation with new feature space and is compared to thresholding, watershed, level set, and active contour techniques.	2 CBCT images	Teeth detection
(Gao & Li, 2013)	The volume data are initially divided into homogeneous blocks and then iteratively merged to produce the initial labeled and unlabeled instances for semi-supervised study.	N.A	Teeth detection
(Ji, Ong & Foong, 2014)	The study adds a new level set procedure for extracting the contour of the anterior teeth. Additionally, the proposed method integrates the objective functions of existing level set methods with a twofold intensity model.	10 CBCT images	Teeth structure
(Hu et al., 2014)	Otsu and mean thresholding technique combinedly used to improve the Segmentation.	Image dataset consists of 300 layers	Teeth detection

Table 4(on next page)

The table shows relevant review findings of conventional machine learning algorithms for different imaging modalities

Table 1 The table shows relevant review findings of conventional machine learning algorithms for different imaging modalities

Author & Year	Relevant review findings	Images	Feature classifier	Detection
Imaging modality: Periapical X-rays				
(Li et al., 2005, 2007)	To segment the dental Image into normal, abnormal, and potentially abnormal areas, the variational level set function is used..	60 X-rays	Trained SVM is used to characterize the normal and abnormal regions after Segmentation.	Bone loss & root decay
Imaging modality: Panoramic X-rays				
(Pushparaj et al., 2013)	The geometrical features are used to classify both premolar and molar teeth, while for tooth numbering, the matching templates method is used effectively.	N.A	Feature extraction (Projected principal edge distribution (PPED) + Geometric properties + Region descriptors) + SVM	Teeth numbering and Classification are used to help Forensic odontologists.
(Sornam & Prabhakaran, 2017)	The Linearly Adaptive Particle Swarm algorithm is developed and implemented to improve the accuracy rate of the neural system classifier.	N.A	Back Propagation Neural Network (BPNN) and Linearly Adaptive Particle Swarm Optimization (LA-PSO)	Caries detection
(Bo et al., 2017)	A two-stage SVM model was proposed for the Classification of osteoporosis.	Dataset consists of 40 images	HOG (histogram of oriented gradients + SVM	Osteoporosis detection
(Vila-Blanco, Tomás & Carreira, 2018)	Segmentation of mandibular teeth carried out by applying Random forest regression-voting constrained local model (RFRV-CLM) in 2 steps: The 1st step gives an estimate of individual teeth and mandible regions used to initialize search for the tooth. In the second step, the investigation is carried out separately for each tooth.	Training images: 261 Testing images: 85	(RFRV-CLMs)	Adult age teeth detection or a missing tooth for person identification.
Imaging Modality: Photographic Color Images				
(Fernandez & Chang, 2012)	Teeth segmentation and Classification of teeth palate using ANN gives better results as compared to SVM. It shows that ANN is 7-times faster than SVM in terms of time	N.A	ANN + Multilayer perceptrons trained with the error back-propagation algorithm.	Oral infecto-contagious diseases,
(Prakash, Gowsika & Sathiyapriya, 2015)	The prognosticating faults method includes the following stages: pre-processing, Segmentation, features extraction, SVM classification, and prediction of diseases.	N.A	Adaptive threshold + Unsupervised SVM classifier	Dental defect prediction
Imaging Modality: CBCT or CT				
(Yilmaz, Kayikcioglu & Kayipmaz, 2017)	Classifier efficiency improved by using the forward feature selection algorithm to reduce the size of the feature vector. The SVM classifier produced the best results in classifying periapical cyst and keratocystic odontogenic tumor (KCOT) lesions.	50 CBCT 3D scans	Order statistics (median, standard deviation, skewness, kurtosis, entropy) and 3D Haralick Features + SVM	Periapical cyst and keratocystic odontogenic tumor
Imaging Modality: Hybrid Dataset Images				
(Nassar & Ammar, 2007)	A hybrid learning algorithm is used to evaluate the binary bayesian classification filters' metrics and the class-conditional intensities.	Bitewing & Periapical films	Feature extraction + Bayesian classification.	Teeth are matching for forensic odontology.
(Avuçlu & Başçiftçi, 2019)	Firstly, Image pre-processing and Segmentation are applied to extract the features and quantitative information obtained from the feature extraction from teeth images. Subsequently, features are used as input to the multilayer perceptron neural network.	1315 Dental X-ray images, 162 different age groups	Otsu thresholding + Feature extraction (average absolute deviation) + Multilayer perceptron neural network	Age and gender classification

Table 5(on next page)

The table shows relevant review findings of deep learning algorithms for different imaging modalities

Table 1 The table shows relevant review findings of deep learning algorithms for different imaging modalities

Authors	Deep learning architectures	Detection/Application	Metrics
Imaging modality: Periapical X-rays			
(Prajapati, Nagaraj & Mitra, 2017)	CNN and transfer learning	Dental caries, periapical infection, and periodontitis	Accuracy:- 0.8846
(Yang et al., 2018)	Conventional CNN	Automated clinical diagnosis	F1 score 0.749
(Zhang et al., 2018)	CNN (label tree with cascade network structure)	Teeth detection & classification	Precision:- 0.958, Recall:- 0.961 F-score :- 0.959
(Choi, Eun & Kim, 2018)	Conventional CNN	Caries detection	F1max:- 0.74 with FPs:- 0.88
(Lee et al., 2018b)	GoogLeNet Inception v3 CNN network	Caries and Non-caries	Premolar Accuracy (premolar):- 0.89, Accuracy(molar):- 0.88, and Accuracy:- 0.82, AUC (premolar):- 0.917, AUC (molar):- 0.890, and an AUC (Both premolar and molar):- 0.845
(Lee et al., 2018a)	CNN (VGG-19)	Periodontally compromised teeth (PCT)	For premolars, the total diagnostic Accuracy(premolars):- 0.810, Accuracy(molars):- 76.7%
(Geetha, Aprameya & Hinduja, 2020)	Back-propagation neural network	Caries detection	Accuracy:- 0.971, FPR:- 0.028, ROC :- 0.987, PRC :- 0.987 with Learning rate:- 0.4, momentum:- 0.2
Imaging modality: Panoramic X-rays			
(Oktay, 2017)	AlexNet	Teeth detection and classification	Accuracy(tooth detection):- 0.90 Classification Accuracy: Molar :-0.9432, Premolar:- 0.9174, Canine & Incisor:- 0.9247
(Chu et al., 2018)	Deep octuplet siamese network (OSN)	Osteoporosis analysis	Accuracy:- 0.898
(Wirtz, Mirashi & Wesarg, 2018)	Coupled shape model + neural network	Teeth detection	Precision:- 0.790, Recall:- 0.827 Dice coefficient:- 0.744
(Jader et al., 2018)	Mask R-CNN model	Teeth detection	Accuracy:- 0.98, F1-score:- 0.88, precision:- 0.94, Recall:- 0.84, and Specificity:- 0.99
(Lee et al., 2019)	Mask R-CNN model	Teeth segmentation for diagnosis and forensic identification	F1 score:- 0.875, Precision:- 0.858, Recall:- 0.893, Mean'IoU':- 0.877
(Kim et al., 2019)	DeNTNet (Deep neural transfer Network)	Bone loss detection	F1 score:- 0.75, Accuracy:- 0.69
(Tuzoff et al., 2019)	R-CNN	Teeth detection and numbering	Tooth detection (Precision:- 0.9945 Sensitivity:- 0.9941) Tooth Numbering (Specificity:- 0.9994, Sensitivity = 0.9800)
(Fukuda et al., 2019)	DetectNet with DIGITS version 5.0	Vertical root fracture	Recall:- 0.75, Precision:- 0.93 F-measure:- 0.83
(Murata et al., 2019)	AlexNet	Maxillary sinusitis	Accuracy:- 0.875, Sensitivity:- 0.867, Specificity:- 0.883, and AUC:- 0.875
(Kats et al., 2019)	ResNet-101	Plaque detection	Sensitivity:- 0.75, Specificity:- 0.80, Accuracy:- 0.83, AUC:- 0.5
(Singh & Sehgal, 2020)	6 - Layer DCNN	Classification of molar, premolar, canine and incisor	Accuracy (augmented database):- 0.95, Accuracy (original database):- 0.92
(Muramatsu et al., 2020)	CNN (Resnet 50)	Teeth detection and classification	Tooth detection sensitivity:- 0.964 Average classification accuracy (single model):- 0.872, (multisized models):- 0.932
(Banar et al., 2020)	Conventional CNN	Teeth detection	Dice score:- 0.93, accuracy:- 0.54, a MAE:- 0.69 , and a linear weighted Cohen's kappa coefficient:- 0.79.
Imaging modality: Bitewing X-rays			
(Srivastava et al., 2017)	Fully convolutional neural network FCNN	Detection of dental caries	Recall:- 80.5, Precision:- 61.5, F-score:- 70.0
Imaging modality: CT & CBCT			
(Miki et al.,	AlexNet architecture	7-Tooth-type classification (canine,	Accuracy:- 0.91

2017a)		molar, premolar, etc.)	
(Miki et al., 2017b)	AlexNet	Teeth detection and classification	Detection accuracy:- 0.774, Classification accuracy:- 0.771
(Hatvani et al., 2018)	Subpixel network + U-Net architecture	Teeth resolution enhancement	Mean of difference (area mm2):- 0.0327 Mean of difference(micrometer):- 114.26 Dice coefficient:- 0.9101
(Torosdagli et al., 2018)	CNN (a long short-term memory (LSTM) network)	Anatomical Landmarking	DSC:- 0.9382
(Egger et al., 2018)	CNN (VGG16, FCN)	Mandible detection	Accuracy:- 0.9877, Dice coefficient:- 0.8964 and Standard deviation:- 0.0169
(Hiraiwa et al., 2019)	AlexNet and GoogleNet	Classification of root morphology (Single or extra)	Diagnostic accuracy:- 0.869
Imaging modality: Hybrid dataset			
(Wang et al., 2016)	U-net architecture (Ronneberger, Fischer & Brox, 2015)	Landmark detection in cephalometric radiographs and Dental structure in bitewing radiographs.	F-score = > 0.7
(Lee, Park & Kim, 2017)	LightNet and MatConvNet	Landmark detection	N.A
(Karimian et al., 2018)	Conventional CNN	Caries detection	Sensitivity:- 97.93~99.85% Specificity:- 100%
Imaging modality: Color images/ Oral images			
(Rana et al., 2017)	Conventional CNN	Detection of inflamed and healthy gingiva	precision:- 0.347, Recall: 0.621, AUC:- 0.746
Image type not defined			
(Imangaliyev et al., 2016)	Conventional CNN	Dental plaque	F1-score:- 0.75

Table 6(on next page)

Performance metrics used by various researchers for the dental image analysis

Table 1 Performance metrics used by various researchers for the dental image analysis

Metric	Symbol	Author's
True positive rate (sensitivity, recall)	<i>TPR</i>	(Hosntalab et al., 2010; Mortaheb, Rezaeian & Soltanian-Zadeh, 2013; Pushparaj et al., 2013; Ghaedi et al., 2014; Abdi, Kasaei & Mehdizadeh, 2015; Berdouses et al., 2015; Datta & Chaki, 2015b; Alsmadi, 2018; Datta, Chaki & Modak, 2019, 2020)
True negative rate (specificity)	<i>TNR</i>	(Hosntalab et al., 2010; Mortaheb, Rezaeian & Soltanian-Zadeh, 2013; Ghaedi et al., 2014; Abdi, Kasaei & Mehdizadeh, 2015; Berdouses et al., 2015; Datta & Chaki, 2015b; Alsmadi, 2018; Datta, Chaki & Modak, 2019)
Positive predictive value (precision)	<i>PPV</i>	(Hosntalab et al., 2010; Mortaheb, Rezaeian & Soltanian-Zadeh, 2013; Pushparaj et al., 2013; Berdouses et al., 2015; Datta, Chaki & Modak, 2020)
Jaccard index	<i>JAC</i>	(Ji, Ong & Foong, 2014)
Dice coefficient	<i>DSC</i>	(Ji, Ong & Foong, 2014; Abdi, Kasaei & Mehdizadeh, 2015; Datta, Chaki & Modak, 2019; Devi, Banumathi & Ulaganathan, 2019)
F-Measure (F1 Measure = Dice)	<i>FMS</i>	(Berdouses et al., 2015; Datta, Chaki & Modak, 2020)
Accuracy	<i>ACC</i>	(Huang & Hsu, 2008; Olsen et al., 2009; Banu et al., 2014; Nuansanong, Kiattisin & Leelasantham, 2014; Ghaedi et al., 2014; Lin et al., 2014; Datta & Chaki, 2015a,b; Poonsri et al., 2016; Rad et al., 2018; Osterloh & Viriri, 2019; Datta, Chaki & Modak, 2019, 2020; Devi, Banumathi & Ulaganathan, 2019; Kumar, Bhadauria & Singh, 2020)
Mahalanobis distance	<i>MHD</i>	(Pushparaj, Gurunathan & Arumugam, 2013)
Hausdorff distance	<i>HD</i>	(Abdi, Kasaei & Mehdizadeh, 2015)
Distance vector	<i>DV</i>	(Prajapati, Desai & Modi, 2012)
Similarity measure	<i>SM</i>	(Pushparaj, Gurunathan & Arumugam, 2013; Alsmadi, 2018; Singh & Agarwal, 2018)
The area under ROC curve	<i>AUC</i>	(Nuansanong, Kiattisin & Leelasantham, 2014)
Cohens kappa coefficient	<i>KAP</i>	(Berdouses et al., 2015)
Mean absolute error	<i>MAE</i>	(Vijayakumari et al., 2012; Amer & Aqel, 2015; Tuan et al., 2018; Kumar, Bhadauria & Singh, 2020)
Mean square error	<i>MSE</i>	(Vijayakumari et al., 2012; Singh & Agarwal, 2018; Tuan et al., 2018)
Error rate	<i>ERR</i>	(Zhou & Abdel-Mottaleb, 2005; Nomir & Abdel-Mottaleb, 2008; Hosntalab et al., 2010; Harandi & Pourghassem, 2011; Lira et al., 2014; Datta & Chaki, 2015b; Purnama et al., 2015; Tuan et al., 2018; Banday & Mir, 2019)
Failure rate	<i>FR</i>	(Said et al., 2006; Al-sherif, Guo & Ammar, 2012)

Table 7 (on next page)

Confusion Matrix

Table 1 Confusion Matrix

<i>True positive rate (Recall/Sensitivity)</i> : It implies how the caries lesion is accurately detected when it is present there.	<i>Sensitivity</i> is expressed as $\frac{TP}{TP + FN}$
<i>True negative rate (Specificity)</i> : That is the amount of negative caries lesion examination when there's no affected lesion.	<i>Specificity</i> is measured as $\frac{TN}{TN + FP}$
<i>Dice Coefficient</i> : This metric measures between two samples.	It is defined as $\frac{2 A \cap B }{(A + B)}$, where $ A $ and $ B $ are the number of elements in the sample.
<i>Accuracy</i> can be defined as the percentage of correctly classified instances.	It is calculated as $\frac{TP + TN}{TP + TN + FN + FP} * 100$.
<i>Precision</i> : It explains the pureness of our positive detections efficiently compared to the ground truth.	It is the positive predictive value defined as $\frac{TP}{TP + FP}$
<i>F-Score</i> : The F-score is a process of combining the model's precision and recall and the harmonic mean of the model's precision and recall.	It is expressed as $2 \times \frac{\text{Precision} \times \text{Recall}}{\text{Precision} + \text{Recall}}$

Table 8(on next page)

Dental X-ray image dataset description for deep Learning

1 Table 1 Dental X-ray image dataset description for deep Learning

Authors & Year	Dataset Description
(Eun & Kim, 2016)	Periapical X-rays: 500 periapical images used for training where each Image is containing five teeth and 100 images used for testing with corresponding ground truth.
(Wang et al., 2016)	Total number of patients: 400 (100 additional patients) Cephalometric radiographs: 400 images .tiff format dimension of 1935 ×2400 pixels, 120 bitewing radiographs (new) (Age group 6 to 60 yrs) Software used: Soredex CRANEXr Excel Ceph machine (Tuusula, Finland) and Soredex SorCom software (3.1.5, version 2.0)
(Prajapati, Nagaraj & Mitra, 2017)	Periapical RadioVisioGraphy (RVG) X-ray: 251 images (labeled dataset) where 180 used for training, 26 images for testing & 45 images validation.
(Rana et al., 2017)	Color images: Training and validation data consist of 258 images & 147 images.
(Lee, Park & Kim, 2017)	300 Dental X-ray images with resolution 1935 x 2400 pixels and 150 images used for training, and 150 images used for testing.
(Srivastava et al., 2017)	Bitewing images: More than 3000 images
(Miki et al., 2017a)	CBCT dataset taken from Asahi University Hospital, Gifu, Japan. 2 dental units: Veraviewepocs 3D (J.Morita Mfg, Corp., Kyoto, Japan) and Alphard VEGA (Asahi Roentgen Ind. Co., Ltd., Kyoto, Japan)
(Miki et al., 2017b)	CT data: 52 images Training group: 42 images, testing group: 10 images
(Oktay, 2017)	Panoramic Images: Dataset taken from 3-different X-ray machines have image dimensions 2871x1577, 1435x791, or 2612x1244 pixels. Testing and validation are done using images of 100 different people.
(Yang et al., 2018)	A small dataset of 196 periapical images used, and also augmentation is performed.
(Zhang et al., 2018)	Periapical Images: Initially for training, 800 images and 200 used for testing. and data is annotated with the help of bounding box labels in 32 teeth position.
(Wirtz, Mirashi & Wesarg, 2018)	Panoramic X-rays: 14 test images used. Image augmentation is used to increase training images up to 4000.
(Choi, Eun & Kim, 2018)	Periapical X-rays: 475 images dimension of 300x413 from 688 × 944 or 1200 × 1650.
(Jader et al., 2018)	Panoramic X-ray images: 193 images used for training containing 6987 teeth and 83 images for validation containing 3040.
(Lee et al., 2018b)	Periapical Images: 3000 images .jpeg format dimension resized to 299x299 pixels The training and validation dataset was 2400 and a test dataset of 600. The training and validation dataset consisted of 1200 dental caries and 1200 non-dental caries, and the test dataset consisted of 300 dental caries and 300 non-dental caries. Augmentation is done up to 10 times for training.
(Hatvani et al., 2018)	Micro CT images: a training set consists of 5680 slices and a test set of 1824 slices was used.
(Torosdagli et al., 2018)	CBCT dataset of 50 patients and qualitative visual inspection were done for 250 patients with high variability.
(Karimian et al., 2018)	Training is performed using different batches containing ten optical coherence tomography (OCT) images per batch.
(Lee et al., 2018a)	Periapical X-ray images resized to 224×224 pixels (from the original 1,440×1,920 pixels) in .png format : For training (n=1,044), validation (n=348), and test (n=348) datasets.
(Egger et al., 2018)	CT dataset containing 45 images as DICOM files with dimension 512x512 from a department of craniomaxillofacial surgery in Austria. 1 st Image set containing 1680 slices, 2 nd one with induced noise images 6720 slices, 3 rd after transformation 13440 slices, and 4 th covered augmentation 18480 slices
(Chu et al., 2018)	Panoramic X-ray: 108 images.
(Hiraiwa et al., 2019)	CBCT images and panoramic radiographs used for 760 mandibular first molars (400 patients)
(Lee et al., 2019)	Panoramic X-rays: Dimensions of 2988 × 1369 pixels. Total 846 annotated tooth images. Training group: 30 radiographs Validation & testing: 20 images. Augmentation technique used to reduce overfitting (obtained 1024 training samples from 846 original data points)
(Kim et al., 2019)	Panoramic Images:12,179 images (annotated by experts) Trained, validated, and tested using 11,189, 190, and 800.
(Tuzoff et al., 2019)	Panoramic radiographs: 1352 images Training group: 1352 images Testing group: 222 images
(Murata et al., 2019)	Panoramic X-rays Total patients: 100 (50 men and 50 women), Training data for 400 healthy and 400 inflamed maxillary sinuses and data augmentation used to make 6000 samples
(Kats et al., 2019)	Panoramic X-ray:65 images and augmentation performed.
(Fukuda et al., 2019)	Panoramic X-ray: 300 images with 900×900 pixels. Training set: 240 images Testing set: 60 images
(Singh & Sehgal, 2020)	Panoramic X-rays: Total 400 images. Training group: 240 images, Testing group: 160 images. Also, augmentation is done by using transformation.

(Muramatsu et al., 2020)	Panoramic X-rays: 100 images dimension of 3000×1500 pixels used for testing and training both.
(Geetha, Aprameya & Hinduja, 2020)	Periapical X-rays: 105 images saved as in .bmp format dimension resized to 256×256 , where caries identified 49 images Training, validation, and testing consists of 49 caries and 56 sound dental X-ray images.
(Banar et al., 2020)	Panoramic(OPGs) image dataset of 400 images used.

2
3